



Aalborg Universitet

AALBORG UNIVERSITY
DENMARK

An IGDT-Stochastic Model for Low-Carbon Economic Dispatch of Integrated Electricity-Natural Gas Systems Considering Grid-Enhancing Technologies

Talebi , Amir ; Agabalaye-Rahvar, Masoud ; Mohammadi-ivatloo, Behnam ; Zare, Kazem;
Anvari-Moghaddam, Amjad

Published in:
IET Generation, Transmission & Distribution

DOI (link to publication from Publisher):
[10.1049/gtd2.13327](https://doi.org/10.1049/gtd2.13327)

Creative Commons License
CC BY 4.0

Publication date:
2024

Document Version
Publisher's PDF, also known as Version of record

[Link to publication from Aalborg University](#)

Citation for published version (APA):

Talebi , A., Agabalaye-Rahvar, M., Mohammadi-ivatloo, B., Zare, K., & Anvari-Moghaddam, A. (2024). An IGDT-Stochastic Model for Low-Carbon Economic Dispatch of Integrated Electricity-Natural Gas Systems Considering Grid-Enhancing Technologies. *IET Generation, Transmission & Distribution*, 18(24), 4042-4064.
<https://doi.org/10.1049/gtd2.13327>

General rights

Copyright and moral rights for the publications made accessible in the public portal are retained by the authors and/or other copyright owners and it is a condition of accessing publications that users recognise and abide by the legal requirements associated with these rights.



- Users may download and print one copy of any publication from the public portal for the purpose of private study or research.
- You may not further distribute the material or use it for any profit-making activity or commercial gain
- You may freely distribute the URL identifying the publication in the public portal -

Take down policy

If you believe that this document breaches copyright please contact us at vbn@aub.aau.dk providing details, and we will remove access to the work immediately and investigate your claim.

ORIGINAL RESEARCH

An IGDT-stochastic model for low-carbon economic dispatch of integrated electricity-natural gas systems considering grid-enhancing technologies

Amir Talebi¹ | Masoud Agabalaye-Rahvar¹  | Behnam Mohammadi-Ivatloo² |
Kazem Zare¹  | Amjad Anvari-Moghaddam³

¹Faculty of Electrical and Computer Engineering, University of Tabriz, Tabriz, Iran

²Department of Electrical Engineering, LUT University, Lappeenranta, Finland

³Department of Energy (AAU Energy), Aalborg University, Aalborg, Denmark

Correspondence

Masoud Agabalaye-Rahvar, Faculty of Electrical and Computer Engineering, University of Tabriz, Tabriz, Iran.

Email: m.agabalaye@tabrizu.ac.ir

Abstract

Utilizing wind power alongside flexible resources such as power-to-gas technology, gas-fuel generator, demand response (DR) program, grid-enhancing technologies, and carbon capture and storage can help to low carbon operation of integrated electricity-gas systems (IEGSs). Accordingly, this paper proposes a low-carbon economic dispatch model for the IEGS, in which gas-fuel generators, DR, and gas-fuel generator are considered to realize the economic and environmentally friendly operation of these systems. Also, the flexible AC transmission system device as one of the grid-enhancing technologies is innovatively included in IEGSs to guarantee that wind power is deliverable entire the electricity system. Besides, power-to-gas equipped with hydrogen storage is used to absorb the excess wind power to produce CH₄. On the other hand, to capture the inherent flexibility of the gas network, the gas-storing characteristic of pipelines is shown by line pack modelling. To manage uncertainties associated with wind power and DR program, the proposed model is formulated as an IGDT-stochastic problem. For efficient computation purposes, the present work follows the mixed-integer linear programming framework. Different case studies are performed on an integrated test system. Numerical simulation results show that the proposed model leads to reducing the total cost, carbon emissions, and wind curtailment by 29%, 16.4%, and 100%, respectively. It can be seen that the proposed low-carbon ED model is environmentally friendly and has economic benefits.

1 | INTRODUCTION

1.1 | Motivations

In recent years, global warming has become one of the most important issues in the world. Research has shown that GHGs (e.g. CO₂ the most common type) are global warming's main cause. So, countries committed to decreasing GHG emissions (Kyoto Protocol) [1]. The power system is one of the main sources of GHG emissions because power units generate large amounts of CO₂. There are different ways to decrease CO₂ emissions in the power system. One way to increase the environmentally friendly and economic power systems operation is the use of REs. REs have no air pollutant emission and their

operation cost is near zero. Hence, REs penetration, particularly WEG, has increased in the power system. However, due to the inherent variability, WEG must be used alongside flexible resources to fully utilize this energy. Flexibility can be captured from the generation side (e.g. GFG and CCS), network side (e.g. GETs and line pack), load side (DR program), and energy storage side (e.g. PtG).

In areas with high WEG penetration, there might not be full access to WEG due to the transmission lines' limitations. This problem can be solved by using GETs. GETs are a group of technologies that increase the transmission of power in existing lines [2]. FACTS devices as one of the GETs can increase the transmission lines' power transfer capacity by modifying their reactance [3]. Another technology for better utilization of

This is an open access article under the terms of the [Creative Commons Attribution-NoDerivs License](https://creativecommons.org/licenses/by-nd/4.0/), which permits use and distribution in any medium, provided the original work is properly cited and no modifications or adaptations are made.

© 2024 The Author(s). *IET Generation, Transmission & Distribution* published by John Wiley & Sons Ltd on behalf of The Institution of Engineering and Technology.

WEG is PtG. This technology absorbs excess power caused by WEG variability and converts it into NG [4]. Using PtG not only causes better utilization of WEG but also is the best tool to reduce power system emissions because absorbs CO₂ in the NG production process [5]. Besides these technologies, utilizing GFG, CCS, and DR program reduces GHG emissions. Using CCS technology with fossil fuel units reduces CO₂ emissions by absorbing and storing CO₂. CCS also provides CO₂ for PtG technology in the methanation process. On the other hand, the DR program can enhance the penetration of WEG by shifting electrical loads from peak periods to off-peak periods.

Deployment of the above-mentioned technologies increases the flexibility of the power system and creates IEGS. Due to the low velocity of NG, gas is stored in pipelines. IEGS can benefit from this characteristic of pipeline which is known as line pack [6].

However, due to the weather conditions and changes in consumer behaviour, the actual response of consumers in the DR program and also the output of WE are uncertain. Unlike the uncertainty of WEG which follows the probability distribution function (PDF), there is no specified PDF for DR uncertainty [7]. Therefore, a suitable hybrid method must be considered to handle the uncertainties of DR and WEG.

1.2 | Literature review

With the installation of the CCS, FFPPs could be converted to CCPPs. Many studies have focused on CCPPs' operation. Reference [8] has investigated the CCPPs' flexibility in the power system operation. The authors in [9] have discussed the CCPPs' operating mechanisms. The CCPP's ability to provide ancillary services has been explored in [10]. Reference [11] has included CCS in the UC problem. Authors of [12] have used CCS to achieve low-carbon ED. Reference [13] has used the DR program and CCS to reduce ship carbon emissions. In these works, WEG's potential has not been considered.

WEG's integration into the power system can further reduce carbon emissions. Reference [14] has integrated WEG and CCS into the ED problem. Authors in [15] have used a stochastic bi-objective model to minimize the cost and emission of a system that includes CCPP, WEG, pumped hydro storage, and DR programs. Additionally, it has considered the electrical consumption and WEG output as uncertainties. With increasing WEG's integration into the power system, a significant WEG output power is spilled due to its variability and technical power system limitations (e.g. insufficient power transfer capacity and ramping up/down limitations). One way to decrease WEG spillage is to use GETs in transmission lines. Dynamic line rating and transmission switching can be mentioned among these technologies [16]. FACTS devices as another type of GETs improve power transfer capacity by controlling line impedance. Reference [17] has applied TCSC-based FACTS devices in stochastic optimal power flow problems to minimize WEG curtailment. Authors of [18] have utilized transmission switching and FACTS devices to flow control in the power lines leading to significant economic savings. Reference [19] has included FACTS devices and

energy storage systems (ESSs) in the UC problem to assess the individual and joint impact on WEG utilization and power system economics. To reduce transmission lines' congestion and increase WEG integration, FACTS devices have been used in [20]. Another reason for WEG curtailment is the insufficient power system ramping. So, PtG technology is a good option for harvesting WEG curtailed power. In addition, due to the CO₂ absorption in CH₄ production process by PtG, this is a promising technology to achieve a low-carbon power system.

On the other hand, GFGs are another widely used technology to help the low-carbon power systems operation. With the deployment of GFGs and PtG, electricity and gas systems are coupled. Therefore, it is imperative to consider a low-carbon model for IEGSs. Low-carbon ED for IEGSs has been addressed in [21–23] taking PtG and CCS into account. Authors of [24] have suggested a day-ahead scheduling model for IEGS with a hybrid AC/DC network. PtG and CCS are integrated into this model to achieve a low-carbon scheme. References [21–24] have not considered uncertainties in their model, while [25] has used the stochastic method to handle WEG uncertainty. In [26] and [27], the CHP unit has been outfitted with CCS and PtG to reduce carbon emissions of an integrated energy system. Reference [26] has not taken uncertainties into account while [27] has applied a distributionally robust approach for handling uncertainties. As well, these works have not considered NG system constraints. Reference [28] has used CCS and DR techniques to decrease carbon emissions in IEGS operations such that a chance-constrained approach has been used to manage the relevant risks. Authors of [29] have proposed a day-ahead and intraday scheduling model for IEGSs under WEG uncertainty. Therefore, to decrease wind curtailment and carbon emissions, CCS, PtG, DR, and EVs facilities have been used. Reference [30] has used a bi-level model to evaluate the impact of multi-energy service providers in IEGS operations. DR programs, energy storage systems, and line packs are used as flexible resources in that work. Authors of [31] have used CCS and electric vehicles to achieve zero emission in the operation of multi-energy systems. Also, a hybrid robust-stochastic method is used in this work to model uncertainties of REs and demand.

1.3 | Research gaps & contributions

So, the following research gaps are seen in the aforementioned reviewed literature:

- In some studies, e.g. references [24–26, 28], PtG has been used individually, while the coordinated operation of PtG with CCS and hydrogen storage can have a significant impact on reducing operation cost and emissions.
- In [11, 15, 19–21, 29, 31], the flexibility that can be obtained from the network side of the IEGS has been ignored. GETs can reduce carbon emissions by increasing wind penetration in power system through increasing power lines' capacity. On the other hand, the line pack characteristic of the gas pipelines can increase the flexibility of the gas system by storing gas in gas pipelines.

TABLE 1 Comparison of the current study and previous studies.

Reference	Scope of study	Flexibility resources						Uncertainties		
		CCS	PtG	Hydrogen storage	GETs	Line pack	DR program	WEG	DR	Uncertainty modelling
[11]	Electricity system	✓	✗	✗	✗	✗	✗	✗	✗	Deterministic
[15]	Electricity system	✓	✗	✗	✗	✗	✓	✓	✗	Stochastic
[18]	Electricity system	✗	✗	✗	✓	✗	✗	✗	✗	Deterministic
[19]	Electricity system	✗	✗	✗	✓	✗	✗	✗	✗	Deterministic
[20]	Electricity system	✗	✗	✗	✓	✗	✗	✓	✗	Robust
[21]	IEGSs	✓	✓	✓	✗	✗	✗	✗	✗	Deterministic
[24]	IEGSs	✓	✓	✗	✗	✗	✗	✗	✗	Deterministic
[25]	IEGSs	✓	✓	✗	✗	✗	✗	✗	✗	Stochastic
[26]	IEGSs	✓	✓	✗	✗	✗	✗	✗	✗	Deterministic
[27]	IEGSs	✓	✓	✓	✗	✗	✗	✓	✗	Distributionally robust
[28]	IEGSs	✓	✗	✗	✗	✗	✓	✓	✗	Chance-constrained
[29]	IEGSs	✓	✓	✓	✗	✗	✓	✓	✗	Stochastic
[30]	IEGSs	✗	✗	✗	✗	✓	✓	✓	✗	Robust
[31]	Multi-energy system	✓	✗	✗	✗	✗	✗	✓	✗	Robust-stochastic
Current study	IEGSs	✓	✓	✓	✓	✓	✓	✓	✓	Hybrid IGDT-Stochastic

- References [15, 28–30] have used the DR program in their model and have not considered the uncertainty associated with DR. Due to the changes in weather conditions and consumer behaviours, actual consumer response to DR programs is uncertain.
- The uncertainty modelling approaches used in references [15, 25, 27–29, 31] are based on PDF. However, there is not always prior knowledge about the PDF of the uncertain parameter.

To cover suitably the above gaps, a low-carbon ED model for IEGSs is proposed considering flexible resources. In addition to the CCS, PtG, and DR program, TCSC-based FACTS devices are included in the proposed model to enhance wind penetration in IEGSs. The line pack characteristic of pipelines is also modelled to enhance the flexibility of the NG system. Using linear models of FACTS devices and gas pipelines, the proposed model follows the MILP framework. Unlike WEG, there is not a specified PDF for DR uncertainty. Hence, a hybrid IGDT-stochastic method is utilized to address uncertainties of WEG and DR. Table 1 shows a comparison of this study with the previous researches. To the best of our knowledge, there is no similar work on evaluating the benefit of mentioned flexible resources in the low-carbon ED of IEGS. As well as it is the first study that addresses the uncertainty of DR in IEGS operation. The contributions are summarized as follows:

- Establishing a coordinated operational model of hydrogen storage, CCS, and PtG technology. On the one hand, PtG uses excess WEG power for NG production. On the other hand, CCS provides the required CO₂ for PtG in the methanation process. As well, hydrogen storage by charging/discharging in required times further decreases cost and emission.

ing/discharging in required times further decreases cost and emission.

- Deploying flexibility provided by the network side of IEGS. GETs are used to enhance the flexibility of the electricity transmission network and WEG penetration level in IEGSs. Also, the line pack is modelled to show the unbalanced relationship between output and input due to the storing capability of pipelines and to enhance the flexibility of the NG network.
- Considering the uncertainty in applying the DR program (i.e. load side flexibility).
- Applying the hybrid IGDT-stochastic method to manage uncertainties of DR and WEG in the proposed low-carbon ED model.

The remaining sections are classified as: Section 2 describes the required components considered in IEGSs with their mathematical modelling. The mathematical formulation of the IGDT-stochastic low-carbon ED model is given in Section 3. Section 4 presents case studies and obtained simulation results. Finally, conclusions are provided in Section 5.

2 | DETAILED SYSTEM DESCRIPTIONS

Flexible resources help IEGS move towards clean and economical operations. Figure 1 shows the flexibility provided by the generation side, network side, load side, and storage side in the IEGS which are employed in this paper. Each mentioned technology is explained with modelling in the following sections. It is worth mentioning that, each of these technologies may be

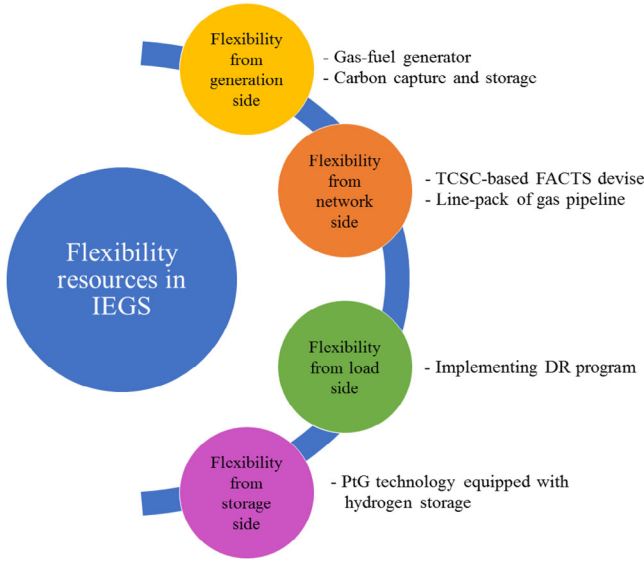


FIGURE 1 Flexibility resources in the proposed IEGS.

owned by different owners however, this paper aims to evaluate their effect on the low-carbon ED of IEGS.

2.1 | Carbon capture and storage (CCS) technology

Three principal methods for CO₂ capture exist, i.e. pre-combustion, oxyfuel combustion, and post-combustion [9]. A detailed description of these methods is found in [32].

The post-combustion CCS system has been taken in this paper. In the following constraints, the superscript X denotes three considered generation unit types (i.e. CPP, CCPP, and GFG), in which the required constraints are defined as Equations (1)–(16) to specify the feasible operating region. The nexus between fuel consumption and power generation is approximated with a linear function. To convert MBTU fuel consumption to kcf unit, it should be used the HHV of NG for gas-based units. The output power limitations are defined as Equation (2) in which the increasing/decreasing capabilities for the output powers amongst two sequential intervals are determined by ramping up/down constraints via Equations (3) and (4). When these units desire to start-up or shut down, fuel consumption should be taken as Equations (5) and (7). It should be noted that these fuel consumptions must be non-negative as Equations (6) and (8). Also, the minimum on/off time linear restrictions are described in Equations (9)–(16). Equations (17) and (18) determine the power units on/off status. According to emission intenseness and power generation, CO₂ emissions can be modelled as Equation (19).

$$\text{FFC}_{i,t} \left(P_{i,t}^{\text{out},X} \right) = \left(\left(a_i P_{i,t}^{\text{out},X} + b_i I_{i,t}^X \right) \right) / \text{HHV}_{\text{gas}}; \quad \forall i \in \psi_X, t \quad (1)$$

$$P_i^{\text{Min},X} I_{i,t}^X \leq P_{i,t}^{\text{out},X} \leq P_i^{\text{Max},X} I_{i,t}^X; \quad \forall i \in \psi_X, t \quad (2)$$

$$P_{i,t}^{\text{out},X} - P_{i,t-1}^{\text{out},X} \leq R_i^{\text{UP},X} (1 - Y_{i,t}) + P_i^{\text{Min},X} Y_{i,t}; \quad \forall i \in \psi_X, t \quad (3)$$

$$P_{i,t-1}^{\text{out},X} - P_{i,t}^{\text{out},X} \leq R_i^{\text{DN},X} (1 - Z_{i,t}) + P_i^{\text{Min},X} Z_{i,t}; \quad \forall i \in \psi_X, t \quad (4)$$

$$\text{SUC}_{i,t}^X = s u_i^X \left(I_{i,t}^X - I_{i,t-1}^X \right); \quad \forall i \in \psi_X, t \quad (5)$$

$$\text{SUC}_{i,t}^X \geq 0; \quad \forall i \in \psi_X, t \quad (6)$$

$$\text{SDC}_{i,t}^X = s d_i^X \left(I_{i,t-1}^X - I_{i,t}^X \right); \quad \forall i \in \psi_X, t \quad (7)$$

$$\text{SDC}_{i,t}^X \geq 0; \quad \forall i \in \psi_X, t \quad (8)$$

$$\sum_{i=1}^{\text{RUP}_i} \left(1 - I_{i,t}^X \right) = 0; \quad \forall i \in \psi_X \quad (9)$$

$$\sum_{i'=t}^{t+\text{MUP}_i-1} I_{i,t'}^X \geq \text{MUP}_i Y_{i,t};$$

$$\forall i \in \psi_X, t = \text{RUP}_i + 1, \dots, \text{NT} - \text{MUP}_i + 1 \quad (10)$$

$$\sum_{i'=t}^{\text{NT}} \left(I_{i,t'}^X - Y_{i,t} \right) \geq 0; \quad \forall i \in \psi_X, t = \text{NT} - \text{MUP}_i + 2, \dots, \text{NT} \quad (11)$$

$$\text{RUP}_i = \min \left\{ \text{NT}, \left(\text{MUP}_i - \text{MUP}_i^{\text{ini}} \right) I_{i,0}^X \right\}; \quad \forall i \in \psi_X \quad (12)$$

$$\sum_{i=1}^{\text{RDN}_i} I_{i,t}^X = 0; \quad \forall i \in \psi_X \quad (13)$$

$$\sum_{i'=t}^{t+\text{MDN}_i-1} \left(1 - I_{i,t'}^X \right) \geq \text{MDN}_i Z_{i,t};$$

$$\forall i \in \psi_X, t = \text{RDN}_i + 1, \dots, \text{NT} - \text{MDN}_i + 1 \quad (14)$$

$$\sum_{i'=t}^{\text{NT}} \left(1 - I_{i,t'}^X - Z_{i,t} \right) \geq 0;$$

$$\forall i \in \psi_X, t = \text{NT} - \text{MDN}_i + 2, \dots, \text{NT} \quad (15)$$

$$\text{RDN}_i = \min \left\{ \text{NT}, \left(\text{MDN}_i - \text{MDN}_i^{\text{ini}} \right) \left(1 - I_{i,0}^X \right) \right\}; \quad \forall i \in \psi_X \quad (16)$$

$$I_{i,t}^X - I_{i,t-1}^X = Y_{i,t} - Z_{i,t}; \quad \forall i \in \psi_X, t \quad (17)$$

$$Y_{i,t} + Z_{i,t} \leq 1; \quad \forall i \in \psi_X, t \quad (18)$$

$$\text{Em}_{i,t}^X = P_{i,t}^{\text{out},X} \eta^X; \quad \forall i \in \psi_X, t \quad (19)$$

With a set ψ_{CCPP} for FFPPs, the same constraints are considered for CCPPs with a set ψ_{CCPP} stated in the above formulations. Regarding CCS integration on CPPs, the feasible region for CCPPs operation can be changed. Due to the consumption of a part of CCPPs' generated power by CCS, CCPPs' net output power is equivalent to the difference between the total output power and CCS consumption expressed in Equation (20). To better comprehend CCS power consumption, Equation (21) is introduced in two parts, i.e. base power and operational power consumptions. The base power consumption is unrelated to the CCS operation status which is assumed as a constant value. Despite most papers ignoring base power consumption due to its lower value rather than the operational power consumption, the aforementioned power is considered in this paper. To treat CO₂ emission in CCS, the required power can be modelled as Equation (22) in which this power is associated with the treated CO₂ using a fixed energy penalty factor. The maximum limit for the treated CO₂ is defined by Equation (23). Due to the operational mechanism, the factual captured CO₂ is not identical to the treated emission. Thus, the capture ratio is considered in Equation (24) to represent the CCS efficiency and capability in capturing treated CO₂. Likewise, the net CO₂ CCPPs' propagation is defined in Equation (25) by the difference between total emission and total CO₂ capture.

$$P_{i,t}^{\text{net,CCPP}} = P_{i,t}^{\text{out,CCPP}} - P_{i,t}^{\text{cons,CCS}}; \quad \forall i \in \psi_{\text{CCPP}}, t \quad (20)$$

$$P_{i,t}^{\text{cons,CCS}} = P_i^{\text{bs,CCS}} + P_{i,t}^{\text{op,CCS}}; \quad \forall i \in \psi_{\text{CCPP}}, t \quad (21)$$

$$P_{i,t}^{\text{op,CCS}} = Em_{i,t}^{\text{tre,CCS}} \gamma^{\text{CCS}}; \quad \forall i \in \psi_{\text{CCPP}}, t \quad (22)$$

$$0 \leq Em_{i,t}^{\text{tre,CCS}} \leq Em_{i,t}^{\text{CCPP}}; \quad \forall i \in \psi_{\text{CCPP}}, t \quad (23)$$

$$P_{t,k}^{\text{FWT}} = \begin{cases} 0; & V_{t,k}^{\text{WT}} < V^{\text{ci}} \text{ or } V_{t,k}^{\text{WT}} \geq V^{\text{co}} \\ \frac{V_{t,k}^{\text{WT}} - V^{\text{ci}}}{V^{\text{rated}} - V^{\text{ci}}} P^{\text{WT,rated}}; & V^{\text{ci}} \leq V_{t,k}^{\text{WT}} < V^{\text{rated}} \\ P^{\text{WT,rated}}; & V^{\text{rated}} \leq V_{t,k}^{\text{WT}} < V^{\text{co}} \end{cases} \quad \forall k \in \psi_{\text{WT}}, t \quad (30)$$

$$Em_{i,t}^{\text{tce}} = Em_{i,t}^{\text{tre,CCS}} \kappa^{\text{CCS}}; \quad \forall i \in \psi_{\text{CCPP}}, t \quad (24)$$

$$Em_{i,t}^{\text{net,CCPP}} = Em_{i,t}^{\text{CCPP}} - Em_{i,t}^{\text{tce}}; \quad \forall i \in \psi_{\text{CCPP}}, t \quad (25)$$

2.2 | Power to gas (PtG) productive technology

A Schematic of PtG with CCS and hydrogen storage is depicted in Figure 2. WEG's excess energy and H₂O is fed into the electrolyser to electrolyzing water [33]. Then, the produced green hydrogen (H₂) is directly used in the methanation facility to

produce NG (CH₄) by Sabatier reaction. The required CO₂ is captured from FFPPs.

To identify the produced H₂ via an electrolyser, Equation (26) is defined. In the methanation process, the required CO₂ and produced CH₄ are computed by Sabatier coefficients according to Equations (27) and (28). The surplus WEG power being utilized in PtG with employed alkaline electrolysis is regarded as the consumption power that must be operated under Equation (29).

$$H_{m,t}^{\text{ptg}} = \frac{P_{m,t}^{\text{ptg}} \eta^{\text{ptg}}}{P_m^{\text{bs,ptg}}}; \quad \forall m \in \psi_{\text{ptg}}, t \quad (26)$$

$$G_{m,t}^{\text{CO}_2} = H_{m,t}^{\text{ptg,M}} \lambda^{\text{H}_2-\text{CO}_2}; \quad \forall m \in \psi_{\text{ptg}}, t \quad (27)$$

$$G_{m,t}^{\text{CH}_4} = H_{m,t}^{\text{ptg,M}} \mu^{\text{H}_2-\text{CH}_4}; \quad \forall m \in \psi_{\text{ptg}}, t \quad (28)$$

$$P_m^{\text{Min,ptg}} \leq P_{m,t}^{\text{ptg}} \leq P_m^{\text{Max,ptg}}; \quad \forall m \in \psi_{\text{ptg}}, t \quad (29)$$

2.3 | Gas-fuel generators (GFGs)

GFGs are another flexible technology that have low pollutant diffusion similar to CCPPs. All needed constraints for GFGs have been clarified in Equations (1)–(19).

2.4 | Wind energy generation (WEG)

Due to the wind speed variability, which affects the optimum results, modelling the output power must be accomplished through different wind speed scenarios. So, the linear scenario-based forecasted power is modelled in Equation (30).

2.5 | Multi-energy storages

As indicated in Figure 2, a CSF is installed among the CCS outlet and the methanation facility, which makes the required CO₂ for the Sabatier reaction. Moreover, an HSF is inserted between the electrolyser and methanation facilities.

To describe the required equations for CSF and HSF, the superscript S denotes these two energy storages. The injection rate of CO₂ (or H₂) from the CCS system (or water electrolysis facility) to the relevant storage is limited by Equation (31)

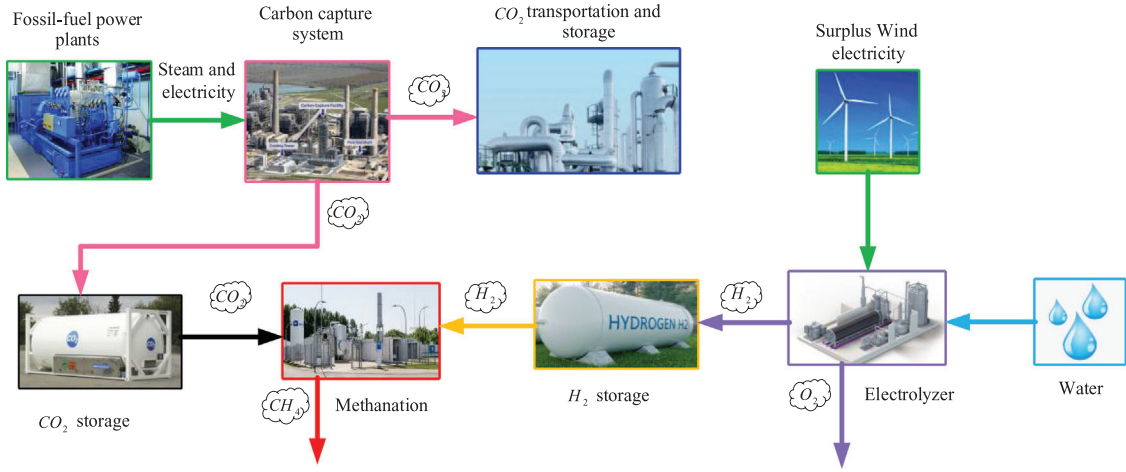


FIGURE 2 Coordination of hydrogen storage, CCS system, and PtG facility to serve a flexible operational model.

whilst the withdrawal rate of CO_2 (or H_2) from the storage to the methanation is restricted by Equation (32). The injected CO_2 is equal to the total captured treated emission by CCPP in Equation (33) and its withdrawal rate from the storage is equal to the required CO_2 for the methanation function in Equation (34). The H_2 injection is equal to the produced amount via an electrolyser in Equation (35) and its withdrawal rate from the storage is equal to the utilized H_2 for the methanation function in Equation (36). To avoid simultaneous injection and withdrawal modes, constraint (37) is taken. The hourly capacity balance of each energy storage regarding injection and withdrawal amounts is determined via Equation (38), which should satisfy the admissible span related to Equation (39). Since the goal of reducing CO_2 as much as possible, the final CSF amount may be less than the initial amount (40); however, the first and final HSF amounts should be equivalent shown in Equation (41).

$$G_s^{\text{S,in,Min}} I_{s,t}^{\text{S,in}} \leq G_{s,t}^{\text{S,in}} \leq G_s^{\text{S,in,Max}} I_{s,t}^{\text{S,in}}, \quad \forall s \in \psi_S, t \quad (31)$$

$$G_s^{\text{S,out,Min}} I_{s,t}^{\text{S,out}} \leq G_{s,t}^{\text{S,out}} \leq G_s^{\text{S,out,Max}} I_{s,t}^{\text{S,out}}, \quad \forall s \in \psi_S, t \quad (32)$$

$$G_{s,t}^{\text{CO}_2,\text{in}} = E m_{i,t}^{\text{tcc}}, \quad \forall s \in \psi_{\text{CSF}}, i \in \psi_{\text{CCPP}}, t \quad (33)$$

$$G_{s,t}^{\text{CO}_2,\text{out}} = G_{m,t}^{\text{CO}_2}, \quad \forall s \in \psi_{\text{CSF}}, m \in \psi_{\text{p2g}}, t \quad (34)$$

$$G_{s,t}^{\text{H}_2,\text{in}} = H_{m,t}^{\text{p2g}}, \quad \forall s \in \psi_{\text{HSF}}, m \in \psi_{\text{p2G}}, t \quad (35)$$

$$G_{s,t}^{\text{H}_2,\text{out}} = H_{m,t}^{\text{p2g,M}}, \quad \forall s \in \psi_{\text{HSF}}, m \in \psi_{\text{p2g}}, t \quad (36)$$

$$I_{s,t}^{\text{S,in}} + I_{s,t}^{\text{S,out}} \leq 1; \quad \forall s \in \psi_S, t \quad (37)$$

$$GL_{s,t}^{\text{S}} = GL_{s,t-1}^{\text{S}} + \left(G_{s,t}^{\text{S,in}} - G_{s,t}^{\text{S,out}} \right) \Delta t; \quad \forall s \in \psi_S, t \quad (38)$$

$$GL_{s,t}^{\text{S,Min}} \leq GL_{s,t}^{\text{S}} \leq GL_{s,t}^{\text{S,Max}}; \quad \forall s \in \psi_S, t \quad (39)$$

$$GL_{s,t=0}^{\text{CO}_2} \geq GL_{s,t=\text{NT}}^{\text{CO}_2}; \quad \forall s \in \psi_{\text{CSF}} \quad (40)$$

$$GL_{s,t=0}^{\text{H}_2} = GL_{s,t=\text{NT}}^{\text{H}_2}; \quad \forall s \in \psi_{\text{HSF}} \quad (41)$$

2.6 | DR program

Various research works defined the DR program to utilize in their optimization models such as [34]. Equation (42) indicates electrical load when the DR program is executed. The amount of load in the DR program is determined by (43). Equation (44) shows load changes in DR in the scheduling horizon is zero. The hourly limit of the DR program is defined in Equation (45).

$$ED_{d,t}^{\text{af}} = ED_{d,t}^{\text{bf}} + edr_{d,t}; \quad \forall d \in \psi_{\text{ED}}, t \quad (42)$$

$$edr_{d,t} = DR_{d,t} ED_{d,t}^{\text{bf}}; \quad \forall d \in \psi_{\text{ED}}, t \quad (43)$$

$$\sum_t edr_{d,t} = 0; \quad \forall d \in \psi_{\text{ED}} \quad (44)$$

$$|DR_{d,t}| \leq DR_{d,t}^{\text{max}}; \quad \forall d \in \psi_{\text{ED}}, t \quad (45)$$

3 | TWO-STAGE STOCHASTIC LOW-CARBON ECONOMIC DISPATCH MODEL

A stochastic low-carbon ED framework is presented through a two-stage model to handle WEG uncertainty appropriately. Besides the considered flexible technologies, various restrictions related to electrical and NG systems are also considered. It is worth mentioning that the linearization process is adopted to linearize the nonlinear gas flow and FACTS devices equations which leads to a MILP formulation along with optimal results.

3.1 | Objective function

The main objective is minimizing the electricity and NG systems' whole cost under a two-stage framework. So, the first line of Equation (46) is taken start-up/shut-down cost of power units. Other parts of Equation (46) are scenario dependent. The second line of Equation (46) is taken as the operational costs of coal-based power plants (i.e. CPPs and CCPPs). The total CO₂ emission cost of non-CCPPs units (i.e. CPPs and GFGs) is defined in the first term of the third line; however, the second term of the third line is relevant to the net CO₂ emission cost of CCPPs. Finally, the extracting NG cost from the corresponding wells is in the first term of the last line and the curtailed electrical demand has a cost denoted in the second term of the last line.

$$\text{Min O.F} = \text{Min} \sum_{t=1}^{\text{NT}} \left(\sum_{i=1}^{\psi_X} \left(\text{SUC}_{i,t}^X + \text{SDC}_{i,t}^X \right) + \sum_{\omega=1}^{\text{NW}} \pi_{\omega} \left(\sum_{i=1}^{\psi_X - \psi_{\text{GFG}}} \left(\text{FFC}_{i,t,\omega} \left(P_{i,t,\omega}^{\text{out},X} \right) \right) + \sum_{i=1}^{\psi_X - \psi_{\text{CCPP}}} \left(\mu^X \left(E m_{i,t,\omega}^X \right) \right) + \sum_{i=1}^{\psi_{\text{CCPP}}} \left(\mu^{\text{CCPP}} \left(E m_{i,t,\omega}^{\text{net,CCPP}} \right) \right) + \sum_{\text{gw}=1}^{\psi_{\text{GW}}} \left(\mu^{\text{ex,gw}} \left(G_{\text{gw},t,\omega}^{\text{ex,gw}} \right) \right) + \sum_{d=1}^{\psi_{\text{ED}}} \sigma^{\text{curt}} \left(E D_{d,t,\omega}^{\text{curt}} \right) \right) \right) \quad (46)$$

3.2 | Constraints

3.2.1 | Power system constraints

In addition to the different sources constraints, i.e. three types of power plants, WEG, PtG, CSF, and HSF facilities described in detail previously, the constraints of the electricity system are specified in the following. The power balance constraint at each bus b and each hour t is denoted in Equation (47). The WEG output power that can be injected into IEGSs must be smaller than the forecasted value which is determined in Equation (48). Constraint (49) limits curtailment of electrical load. A DC power flow is applied in all transmission lines, both with and without FACTS devices' presence, to reduce the computational burden. So, the power flow via simple lines is computed in Equation (50) in which the related limitations should be satisfied as Equation (51). Similar to the power flow computations described in Equations (50) and (51), constraints (52) and (53) are developed to determine power flows via lines equipped with FACTS devices. Despite the susceptance of Equation (50) being a parameter, the susceptance of Equation (52) is a variable due to modifying the reactance. Figure 3 shows a TCSC-based FACTS device that consists of a thyristor-controlled reactor in parallel with a capacitor. As specified in [35], the considered FACTS devices do not vary the flow direction in the transmission lines. To linearize the non-linear (52), a binary variable $x_{i\text{FACTS},t}$ is used to reveal the voltage angle difference sign between two connected buses where if it has the positive sign,

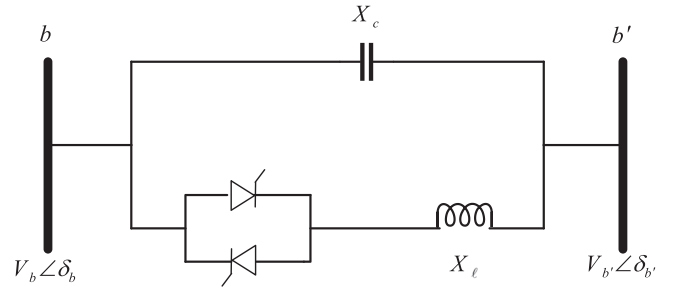


FIGURE 3 TCSC-based FACTS devise.

$x_{i\text{FACTS},t}$ is equal to 1, and the negative sign is stated with $x_{i\text{FACTS},t}$ equal to 0. Thus, the constraints (54)–(59) are clarified how the

non-linear transformation process is handled through the introduced $x_{i\text{FACTS},t}$ and the Big-M method. In order to specify the greater bus between two buses in each transmission line, constraints (58) and (59) are employed concerning a binary variable $x_{i\text{FACTS},t}$. Selecting the best value for the constant M in the Big-M method is done via the maximization term in Equation (60). For all buses except the slack bus, the voltage angles should be maintained within the range $[-\pi, \pi]$ of Equation (61); however, the voltage angle of the slack bus is set to 0 denoted in Equation (62).

$$\sum_{i=1}^{\text{NCGPP}^b} P_{i,t,\omega}^{\text{out},X} + \sum_{i=1}^{\text{NCCPP}^b} P_{i,t,\omega}^{\text{net,CCPP}} + \sum_{k=1}^{\text{NWT}^b} P_{t,k,\omega}^{\text{WT}} - \sum_{m=1}^{\text{Np2g}^b} P_{m,t,\omega}^{\text{p2g}} - \sum_{l=1|m(l)}^{\text{NL}^b} p f_{l,t,\omega} + \sum_{l=1|n(l)}^{\text{NL}^b} p f_{l,t,\omega} = \sum_{d=1}^{\text{NED}^b} \left(E D_{d,t,\omega}^{\text{af}} - E D_{d,t,\omega}^{\text{curt}} \right) \quad \forall b \in \psi_B, t, \omega \quad (47)$$

$$0 \leq P_{t,k,\omega}^{\text{WT}} \leq P_{t,k}^{\text{FWT}}; \quad \forall k \in \psi_{\text{WT}}, t, \omega \quad (48)$$

$$0 \leq E D_{d,t,\omega}^{\text{curt}} \leq E D_{d,t}; \quad \forall d \in \psi_{\text{ED}}, t, \omega \quad (49)$$

$$p f_{l,t,\omega} = B_l^{\text{sus}} (\delta_{b,t,\omega} - \delta_{b',t,\omega}); \quad \forall b, b' \in \psi_B, l \in \psi_L, t, \omega \quad (50)$$

$$-p f_l^{\text{Max}} \leq p f_{l,t,\omega} \leq p f_l^{\text{Max}}; \quad \forall l \in \psi_L, t, \omega \quad (51)$$

$$pf_{l^{\text{FACTS}},t,\omega} = B_{l^{\text{FACTS}},\omega}^{\text{sus}} (\delta_{b,t,\omega} - \delta_{b',t,\omega});$$

$$\forall b, b' \in \psi_B, l^{\text{FACTS}} \in \psi_{L^{\text{FACTS}},t,\omega} \quad (52)$$

$$B_{l^{\text{FACTS}}}^{\text{sus,Min}} \leq B_{l^{\text{FACTS}},\omega}^{\text{sus}} \leq B_{l^{\text{FACTS}}}^{\text{sus,Max}}, \quad \forall l^{\text{FACTS}} \in \psi_{L^{\text{FACTS}},t,\omega} \quad (53)$$

$$pf_{l^{\text{FACTS}},t,\omega} \geq \alpha_{l^{\text{FACTS}},t} B_{l^{\text{FACTS}}}^{\text{sus,Min}} (\delta_{b,t,\omega} - \delta_{b',t,\omega})$$

$$- (1 - \alpha_{l^{\text{FACTS}},t}) M; \quad \forall b, b' \in \psi_B, l^{\text{FACTS}} \in \psi_{L^{\text{FACTS}},t,\omega} \quad (54)$$

$$pf_{l^{\text{FACTS}},t,\omega} \geq (1 - \alpha_{l^{\text{FACTS}},t}) B_{l^{\text{FACTS}}}^{\text{sus,Max}} (\delta_{b,t,\omega} - \delta_{b',t,\omega})$$

$$- \alpha_{l^{\text{FACTS}},t} M; \quad \forall b, b' \in \psi_B, l^{\text{FACTS}} \in \psi_{L^{\text{FACTS}},t,\omega} \quad (55)$$

$$pf_{l^{\text{FACTS}},t,\omega} \leq \alpha_{l^{\text{FACTS}},t} B_{l^{\text{FACTS}}}^{\text{sus,Max}} (\delta_{b,t,\omega} - \delta_{b',t,\omega})$$

$$+ (1 - \alpha_{l^{\text{FACTS}},t}) M; \quad \forall b, b' \in \psi_B, l^{\text{FACTS}} \in \psi_{L^{\text{FACTS}},t,\omega} \quad (56)$$

$$pf_{l^{\text{FACTS}},t,\omega} \leq (1 - \alpha_{l^{\text{FACTS}},t}) B_{l^{\text{FACTS}}}^{\text{sus,Min}} (\delta_{b,t,\omega} - \delta_{b',t,\omega})$$

$$+ \alpha_{l^{\text{FACTS}},t} M; \quad \forall b, b' \in \psi_B, l^{\text{FACTS}} \in \psi_{L^{\text{FACTS}},t,\omega} \quad (57)$$

$$\delta_{b,t,\omega} + (1 - \alpha_{l^{\text{FACTS}},t}) M \geq \delta_{b',t,\omega};$$

$$\forall b, b' \in \psi_B, l^{\text{FACTS}} \in \psi_{L^{\text{FACTS}},t,\omega} \quad (58)$$

$$\delta_{b',t,\omega} + \alpha_{l^{\text{FACTS}},t} M \geq \delta_{b,t,\omega};$$

$$\forall b, b' \in \psi_B, l^{\text{FACTS}} \in \psi_{L^{\text{FACTS}},t,\omega} \quad (59)$$

$$M > \max \{ pf_{l^{\text{FACTS}},t,\omega} + B_{l^{\text{FACTS}}}^{\text{sus}} (\delta_{b',t,\omega} - \delta_{b,t,\omega}) \};$$

$$\forall b, b' \in \psi_B, l \in \psi_L, t, \omega \quad (60)$$

$$-\pi \leq \delta_{b,t,\omega}, \delta_{b',t,\omega} \leq \pi; \quad \forall b, b' \in \psi_B \setminus b, b' : \text{Ref.bus}, t, \omega \quad (61)$$

$$\delta_{r,t,\omega} = 0; \quad r : \text{Ref.bus}, \forall t, \omega \quad (62)$$

3.2.2 | Natural gas system constraints

In Equation (63), the gas flow description is realized via the Weymouth non-linear equation which depends on the pressure at the vicinal nodes, pipeline physical attributes, and gas volumetric feature. Due to the non-linearity and non-convexity of Equation (63), the Taylor series expansion method around fixed pressure points (FPPs) is utilized to linearize it [36]. The pipeline's pressure at each node must be maintained within the predetermined limits as Equation (64) to assure a secure system

operation. Based on the adopted linearized approach via [36], Equation (63) is substituted by a linear inequality presented in Equation (65) which the set of FPPs denoted by $(pr_{e,\vartheta}^{\text{ct}}, pr_{f,\vartheta}^{\text{ct}})$. The linear statements employed in Equation (65) are adjusted based on FPPs which belong to the pressure limits of two vicinal nodes. So, here generating these pressure points is done by selecting various pressure values of the vicinal nodes between their respective limits. To explain the detailed bidirectional gas flows linearization refer to [37]. A very important characteristic of gas pipelines is their ability to store natural gas, which is known as a line pack. Considering the line pack characteristic of the pipeline enhances the flexibility of the NG system. Line pack is modelled through Equations (66)–(68). Equation (66) defines gas flow as the average of outflow and inflow to the pipeline. Equations (67) and (68) show that the line pack of the pipeline is related to the average pressure and inflow and outflow of the pipeline. The NG supply and demand constraint at each node e and each hour t is provided in Equation (69). Also, the NG extracting from the corresponding wells has specific limitations defined in Equation (70).

$$G_{ef,t,\omega} = \kappa_{ef}^{\text{ct}} \sqrt{pr_{e,t,\omega}^2 - pr_{f,t,\omega}^2}; \quad \forall (e, f) \in \psi_Z, t, \omega \quad (63)$$

$$pr_e^{\text{Min}} \leq pr_{e,t,\omega} \leq pr_e^{\text{Max}}; \quad \forall e \in \psi_E, t, \omega \quad (64)$$

$$G_{ef,t,\omega} \leq \kappa_{ef}^{\text{ct}} \left[\frac{pr_{e,\vartheta}^{\text{ct}}}{\sqrt{(pr_{e,\vartheta}^{\text{ct}})^2 - (pr_{f,\vartheta}^{\text{ct}})^2}} pr_{e,t,\omega} - \frac{pr_{f,\vartheta}^{\text{ct}}}{\sqrt{(pr_{e,\vartheta}^{\text{ct}})^2 - (pr_{f,\vartheta}^{\text{ct}})^2}} pr_{f,t,\omega} \right];$$

$$\forall (e, f) \in \psi_Z, \vartheta \in \psi_V, t, \omega \quad (65)$$

$$G_{ef,t,\omega} = \frac{G_{ef,t,\omega}^{\text{in}} + G_{ef,t,\omega}^{\text{out}}}{2}; \quad \forall (e, f) \in \psi_Z, t, \omega \quad (66)$$

$$L_{ef,t,\omega} = \kappa_{ef}^{\text{lp}} \frac{pr_{e,t,\omega} + pr_{f,t,\omega}}{2}; \quad \forall (e, f) \in \psi_Z, t, \omega \quad (67)$$

$$L_{ef,t,\omega} = L_{ef,t-1,\omega} + G_{ef,t,\omega}^{\text{in}} - G_{ef,t,\omega}^{\text{out}};$$

$$\forall (e, f) \in \psi_Z, t, \omega \quad (68)$$

$$\sum_{gw=1}^{\text{NGW}^e} G_{gw,t,\omega}^{\text{ex,gw}} + \sum_{m=1}^{\text{Np2g}^e} G_{m,t,\omega}^{\text{CH}_4} = \sum_{i=1}^{\text{NGFG}^e} \text{FFC}_{i,t,\omega} (P_{i,t,\omega}^{\text{out,GFG}})$$

$$+ \sum_{g=1}^{\text{NGD}^e} GD_{g,t} + \sum_{j=1}^{\text{NZ}^e} (G_{ef,t,\omega}^{\text{in}} - G_{ef,t,\omega}^{\text{out}}); \quad \forall e \in \psi_E, t, \omega \quad (69)$$

$$G_{gw}^{\text{ex,gw,Min}} \leq G_{gw,t,\omega}^{\text{ex,gw}} \leq G_{gw}^{\text{ex,gw,Max}}; \quad \forall gw \in \psi_{\text{GW}}, t, \omega \quad (70)$$

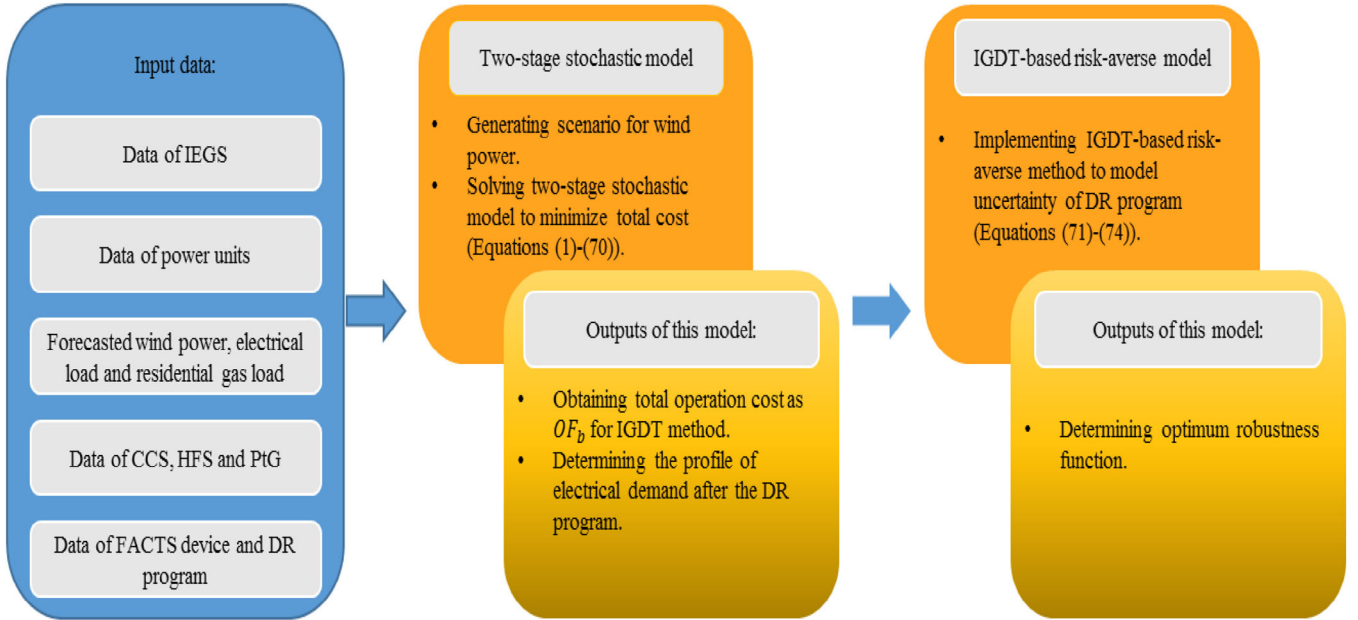


FIGURE 4 The proposed model.

4 | HYBRID IGDT-STOCHASTIC LOW-CARBON ECONOMIC DISPATCH MODEL

In this section, the uncertainty posed by the DR program is modelled with the IGDT method. The PDF of the wind speed is certain, which is Weibull. However, the PDF of the DR program is not known. So, the uncertainty modelling of wind speed is done via the stochastic method, however, the uncertainty of the DR program is accomplished by the IGDT approach, which only uses the uncertainty radius. With these explanations, we cannot apply only the stochastic method for the whole uncertainties in IEGSs, thus deploying the hybrid IGDT-stochastic approach is necessary. IGDT approach has the advantage over the stochastic method because it does not require PDF of uncertain parameters [34]. So it is suitable for modelling DR uncertainty (because it does not have a specified PDF). The IGDT method utilizes two strategies to manage uncertainty: risk-averse and risk-taker [38]. In this paper, the risk-averse strategy is utilized to model the uncertainty of DR.

Uncertainty of DR in the risk-averse strategy is modelled in a way that would result in higher total cost. Since an increase in electrical load in the DR program leads to a higher total cost of IEGS, the IGDT-based risk-averse model can be formulated as Equations (71)–(74). ξ and α are uncertainty radius and robustness function, respectively. Also, Δr is the cost deviation factor that is determined by the system operator.

$$\alpha = \max \xi \quad (71)$$

$$OF \leq (1 + \Delta r) \cdot OF_B \quad (72)$$

$$\begin{aligned} & \sum_{i=1}^{NCGPP^b} P_{i,t,\omega}^{out,X} + \sum_{i=1}^{NCCPP^b} P_{i,t,\omega}^{net,CCPP} + \sum_{k=1}^{NWT^b} P_{t,\kappa,\omega}^{WT} - \sum_{m=1}^{Np2g^b} P_{m,t,\omega}^{p2g} \\ & - \sum_{l=1|m(l)}^{NL^b} p f_{l,t,\omega} + \sum_{l=1|n(l)}^{NL^b} p f_{l,t,\omega} = \quad ; \\ & \sum_{d=1}^{NED^b} \left((1 + \xi) \cdot ED_{d,t,\omega}^{af} - ED_{d,t,\omega}^{curr} \right) \\ & \forall b \in \psi_B, t, \omega \quad (73) \end{aligned}$$

$$\text{s.t. Equations (1) – (41) and (48) – (70).} \quad (74)$$

The simulation process of the proposed model is depicted in Figure 4. As shown in this figure, OF is obtained by solving the stochastic model. Also, in this stage, the profile of electrical load demand is changed based on the DR program. By solving the stochastic model, OF and ED^{af} are sent to the IGDT model as the output of the stochastic model. Finally, the IGDT-based risk-averse model is solved by considering OF_B in (72) and ED^{af} in Equation (73) as parameters.

5 | SIMULATION RESULTS AND DISCUSSIONS

5.1 | 6-bus power system with 6-node gas network

The proposed model is applied on a 6-bus power system/6-node NG network as a small-scale IEGS. The proposed system is depicted in Figure 5 [39]. The gas network contains two gas wells, four loads (i.e. three residential consumptions and GFGs usage), and five pipelines. The power system contains

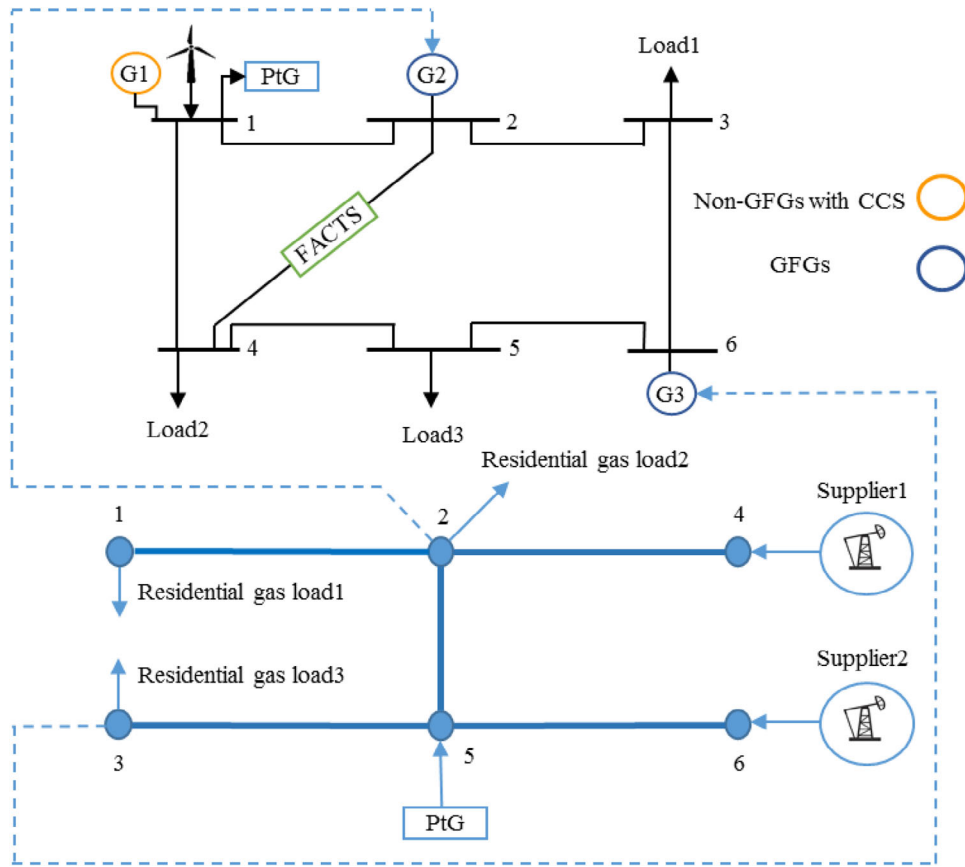


FIGURE 5 Small-scale test system.

seven transmission lines, three loads, one WEG, and three generators. The carbon emission coefficients for GFGs (i.e. G2 and G3) and non-GFGs (i.e. G1) are $0.65 \text{ tCO}_2/\text{MWh}$ and $0.85 \text{ tCO}_2/\text{MWh}$, respectively [14]. As well, G1 has the highest generation capacity that is outfitted with CCS to reduce this generator's emissions. The CCS carbon capture rate is set to 90% and the power consumption for the carbon treatment is set to $0.27 \text{ MWh}/\text{tCO}_2$ [25]. The carbon emission's price is equal to $20 \text{ \$/tCO}_2$ [25]. The PtG is located in node 5 and bus 1 of the gas network and power system, respectively. The data of the power system and gas network are given in the Tables A1–A3. The hourly gas and electrical loads, as well as predicted WEG power, are shown in Figure 6. Other required data for the proposed system is found in references [39] and [29].

The proposed model's effectiveness is evaluated through the following case studies:

- Case 1:** stochastic low-carbon ED of IEGS without CCS, PtG, DR, and TCSC-based FACTS device.
- Case 2:** Case 1 with TCSC-based FACTS device.
- Case 3:** Case 1 with CCS and PtG technologies.
- Case 4:** Case 1 with DR program.
- Case 5:** Case 1 with CCS, PtG, DR, and TCSC-based FACTS device.

Case 6: IGDT-stochastic low carbon ED of IEGS with flexible resources.

CPLEX solver in GAMS software is utilized to solve case studies. The WEG's initial scenarios are generated by the Monte-Carlo method and then reduced through a fast-forward approach via the SCENRED tool in GAMS software.

Case 1: This is a base case and is considered to show how the integration of CCS, PtG, DR, and FACTS devices in the following cases can help the environmental and economic IEGS operation. The various generators' total carbon emissions are 2909.1 tCO_2 . Also, 259.6 MWh of WEG is curtailed due to insufficient power line loadability and ramping limitations. In addition, between 12–21 h (peak period) 93.1 MWh of the electrical load is curtailed which is the reason is the insufficient transmission lines' loadability. Therefore, it can be said that the limited power lines' loadability not only causes WEG curtailment but also leads to electrical load shedding.

As stated previously, considering the line pack characteristic of the gas system increases the flexibility of the gas network due to the unbalanced relationship between output and input. Figure 7 shows the output of gas wells without and with a line pack of pipelines. According to this figure, without considering the line pack, the output of gas wells accurately equals gas demand. While, by considering the line pack characteristic, the

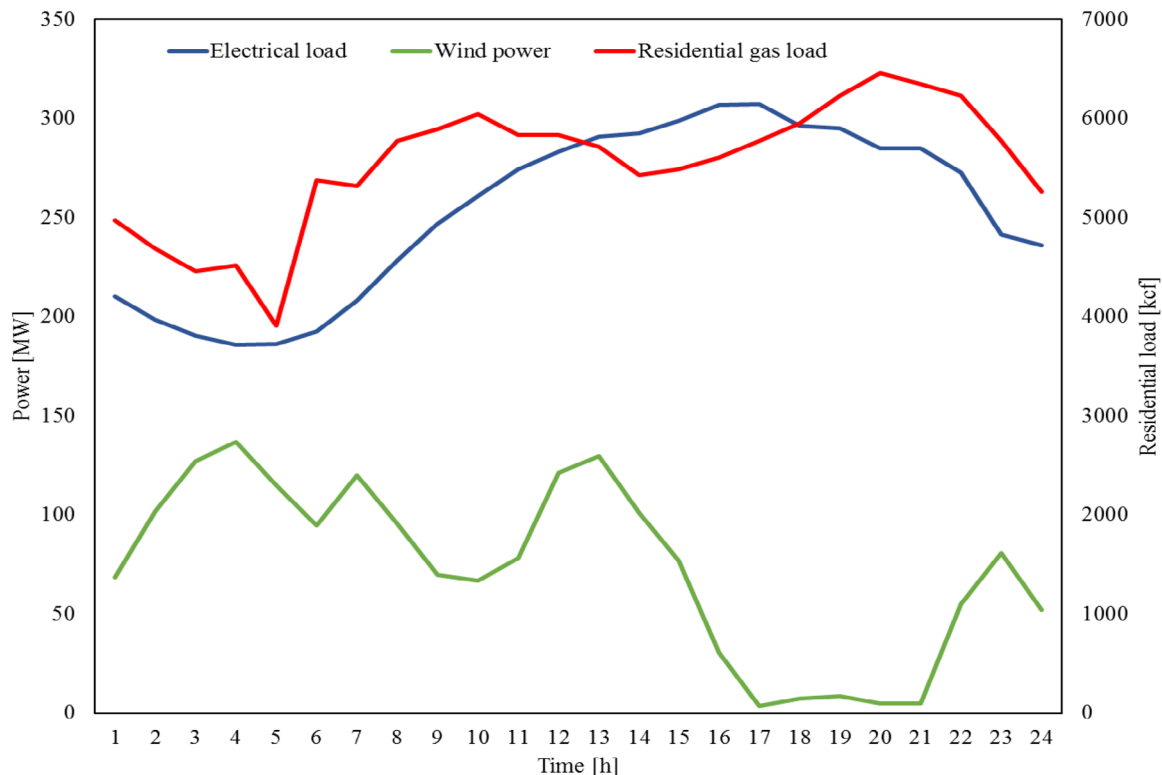


FIGURE 6 Electrical load, WEG, and residential gas load profiles.

TABLE 2 Comparison of total cost and load shedding of IEGS without/with line pack.

	With line pack	Without line pack
Total cost (\$)	424167.63	428986.7
Load shedding (MWh)	132.36	135.6

gas demand is met with wells and line pack. In order to further analyse the effect of the line pack of gas pipelines in the operation of IEGS, we increased the residential gas load by 10%. Table 2 shows that taking line pack characteristics into account reduces total cost and load shedding in IEGS.

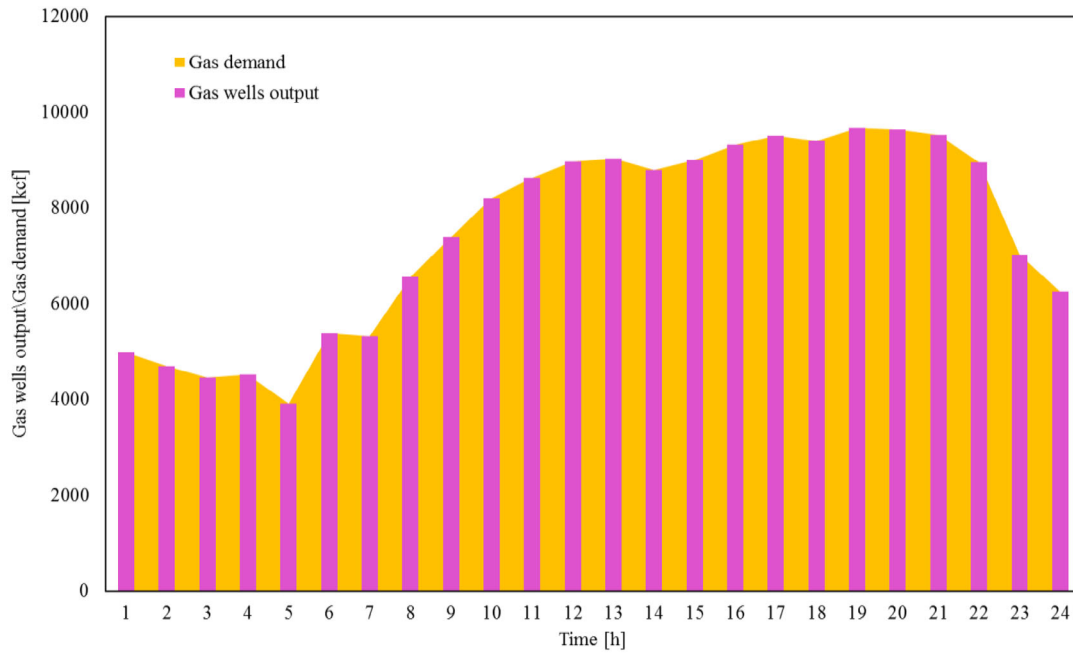
Case 2: The effect of the TCSC-based FACTS device on the proposed model is evaluated in this case. This device is installed on line 2–4. The maximum ratio reactance changes of the transmission line with the FACTS device is assumed to be 40% means it can increase or decrease reactance up to 40%. Figure 8 shows the power flow comparison in line 2–4 (transmission line with FACTS device) in the base case and this case. As shown the FACTS device has increased the proposed transmission line's power transfer capacity. Table 3 presents the reactance changes resulting from the FACTS device, which it can be concluded that under a high range of reactance changes, the total cost, WEG curtailment, and electric load shedding are further reduced. However, individual FACTS device utilization cannot accommodate all WEG power. It should be noted that with increasing transmission line loadability through the FACTS device, the power units' production has increased. Hence, car-

TABLE 3 Results of Case 2.

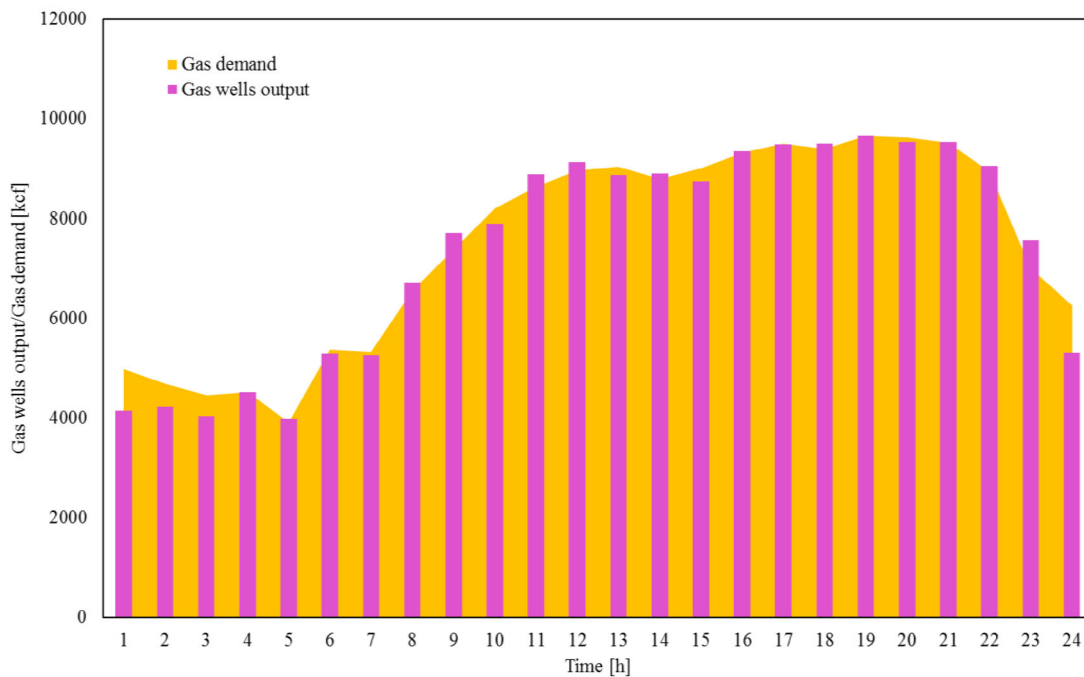
Reactance changes (%)	Total cost (\$)	Total emission (tCO ₂)	WEG curtailment (MWh)	Electrical load shedding (MWh)
10	340705.7	2921.5	245.6	59.9
20	312474.7	2931.1	232.4	32.05
30	291534.7	2934.9	218.1	11.85
40	278725.15	2930.9	200.9	0.73

bon emissions have also increased. The hourly scheduling of G1 in Cases 1 and 2 is shown in Figure 9. The total production of G1 in Cases 1 and 2 is 3002.5 and 3162.2 MWh, respectively.

Case 3: The test system is equipped with coordinated CCS and PtG technologies. So, captured and stored carbon by CCS can be used by PtG in the methanation process. On the other hand, PtG absorbs the excess WEG power and converts it to hydrogen, and stores it in the respective storage. In this regard, PtG absorbs 193.3 MWh excess WEG power for the electrolysis process. It is worth mentioning that, integrating HSF in the PtG leads to more benefit for IEGSs. Table 4 shows the results of Case 3 with and without HSF. Using HSF, PtG produces CH₄ when electrical and gas loads are high and pipelines do not have sufficient capacity. It can also be concluded that PtG cannot prevent electrical load curtailment. PtG's output methane with and without HSF is represented in Figure 10. As aforementioned, in the HSF presence, PtG produces CH₄ when the gas load is



(a)



(b)

FIGURE 7 Gas wells output and gas demand: (a) without line pack, (b) with line pack.

TABLE 4 Results of Case 3.

Case 3	Total cost (\$)	Total emission (tCO ₂)	Electrical load shedding (MWh)
Without HSF	367902.1	2458.5	93.2
With HSF	365827.8	2432.3	93.16

high or the gas pipelines do not have sufficient capacity (i.e. 8, 17, 19, 22, and 24 h). On the other hand, without HSF, PtG directly converts absorbed WEG to CH₄ (3–5, 7, and 12–14 h). Figure 11 shows the effect of CCS on WEG curtailment. Due to the CCS power consumption, WEG curtailment is reduced compared to Case 1. So it can be said that CCS increases WEG penetration.

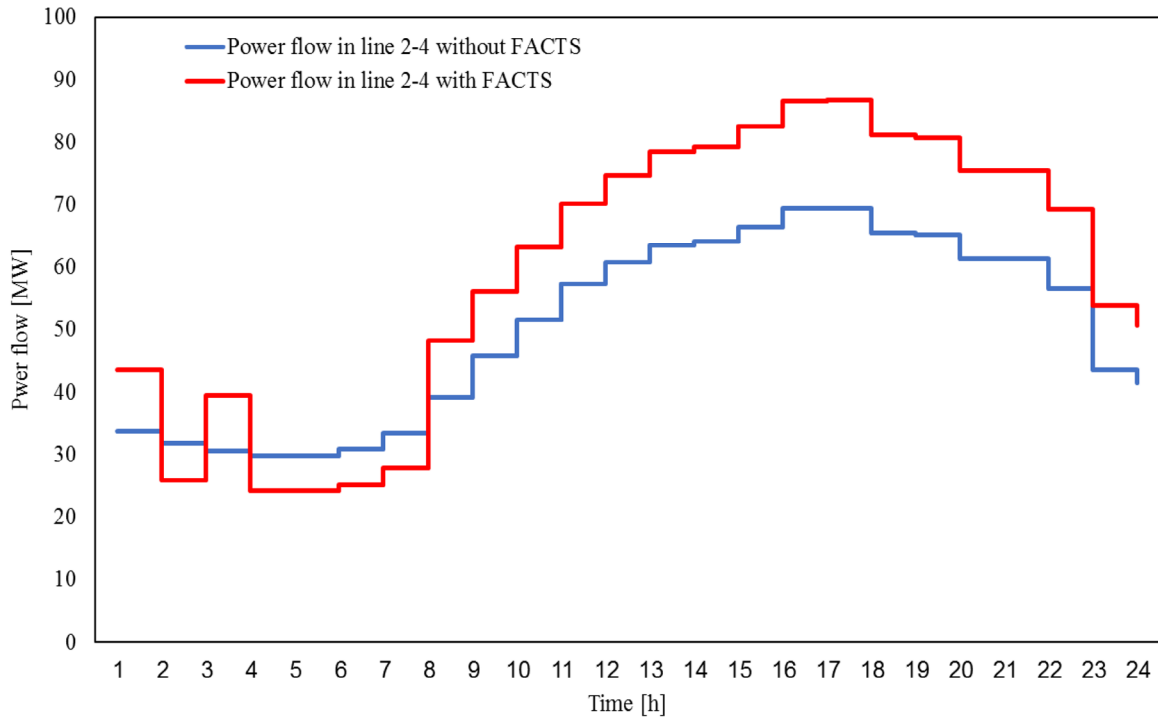


FIGURE 8 Power flow in line 2–4 without/with FACTS device.

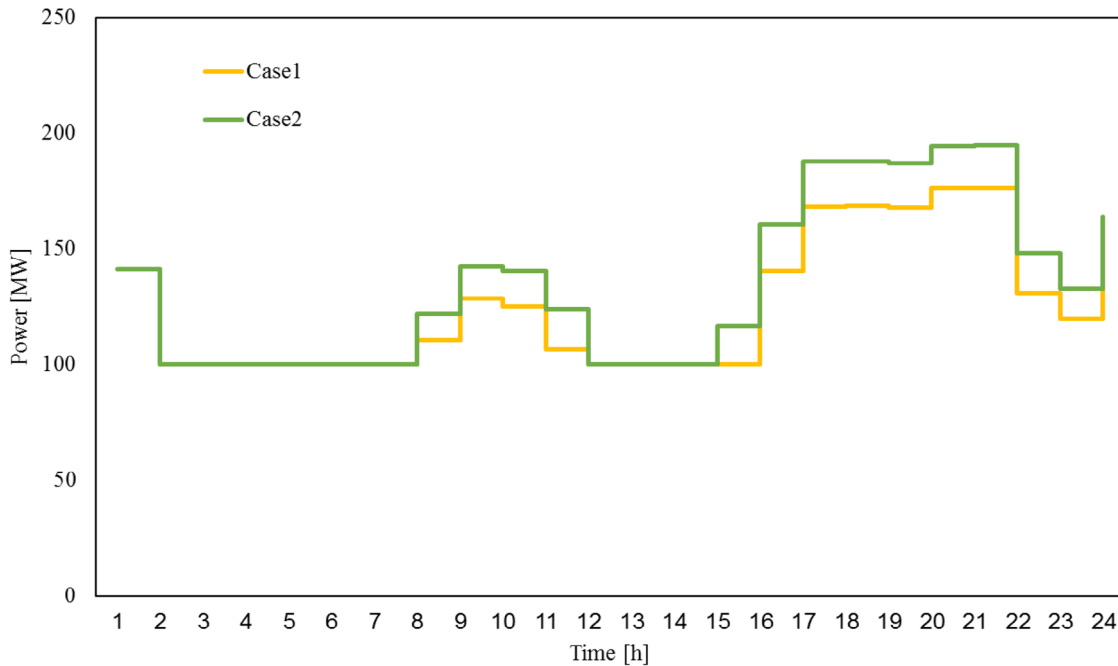


FIGURE 9 The hourly production of G1 in Cases 1 and 2.

Case 4: The DR program is executed in the load buses of the electrical system in this case. The participation rate of electrical loads in this program is set to 5%. In comparison with Case 1, the amount of WEG curtailment and load shedding has decreased to 198.8 and 20.3 MWh, respectively. However, the amount of total carbon emissions has increased to 2916.9 tCO₂. The reason is that the amount of load shedding has reduced.

Figure 12 shows the effect of the DR program on the line pack of the pipeline between nodes 5 and 6. This figure demonstrates that the line pack of the pipeline is more utilized with the DR program. Table 5 gives the simulation results of this case under different participation rates. The outcomes demonstrate that increasing the participation rate of consumers can help the economic and environmentally-friendly operation of IEGS.

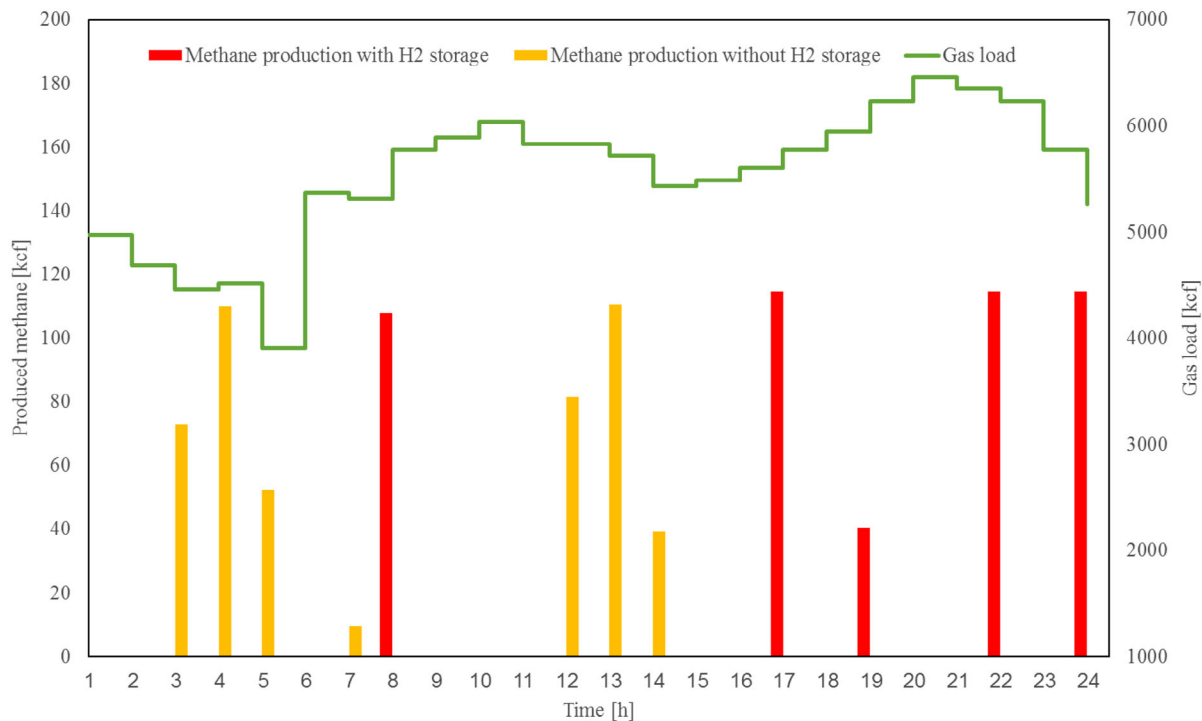


FIGURE 10 PtG output methane with and without hydrogen storage.

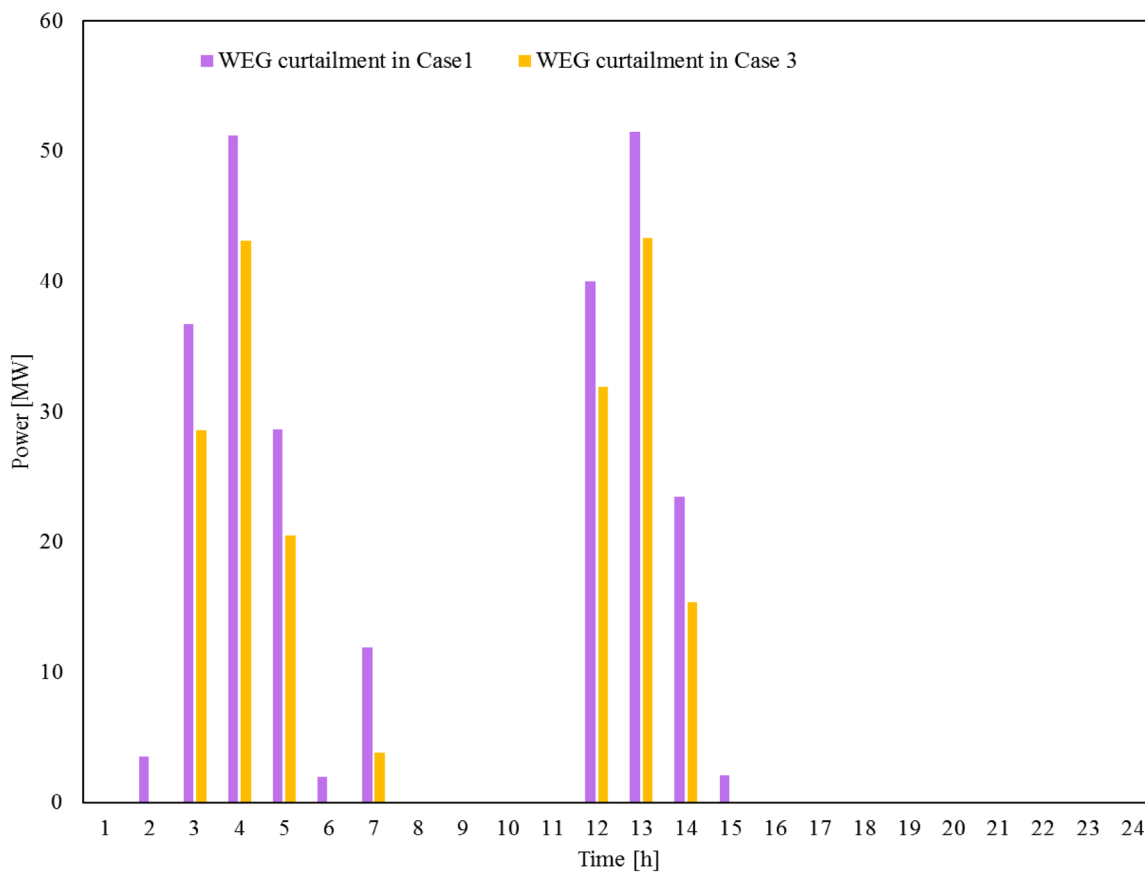


FIGURE 11 WEG curtailment in Cases 1 and 3.

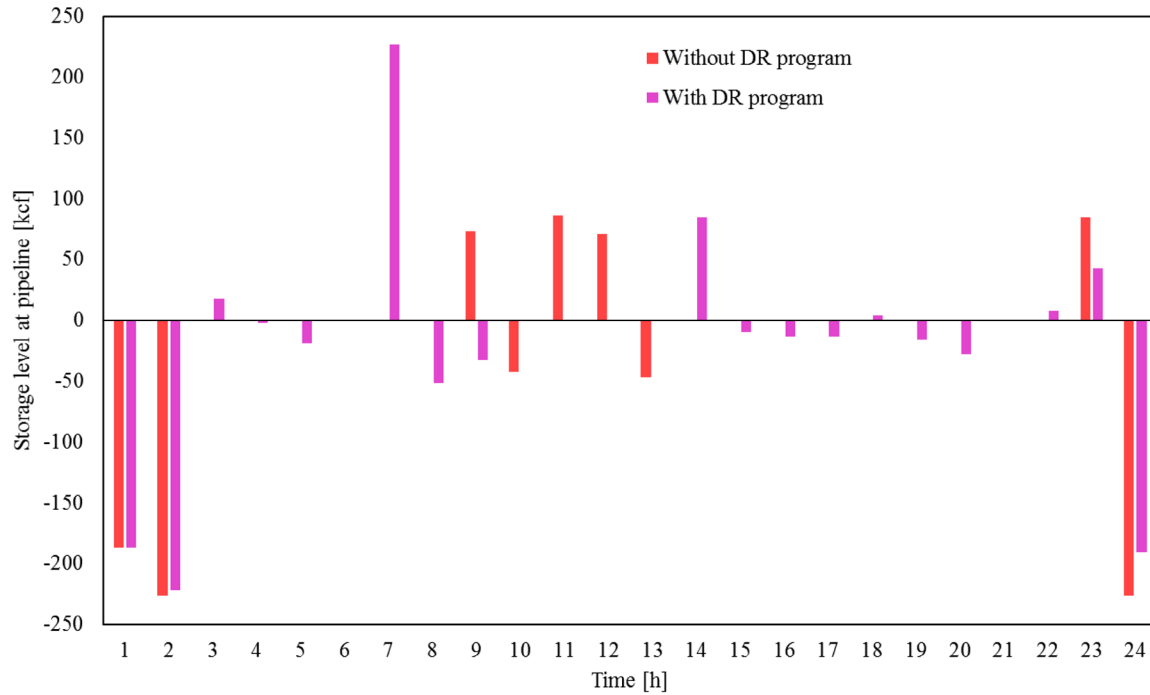


FIGURE 12 Storage level at pipeline 4–6 without and with DR program.

TABLE 5 Results of Case 4 for different participation rates.

Participation rate (%)	Total cost (\$)	Total emission (tCO ₂)	WEG curtailment (MWh)	Electrical load shedding (MWh)
3	324801.7	2914.7	217.8	43.7
5	301324.9	2916.9	198.8	20.2
7	288236.5	2914	183.1	7.8
10	279201.4	2901.1	154.1	0

TABLE 6 Comparison results of five cases.

Case	Total cost (\$)	Total emission (tCO ₂)	WEG curtailment (MWh)	Electrical load shedding (MWh)
1	374136.9	2909.1	259.6	93.1
2	278725.1	2930.9	200.9	0.72
3	365827.8	2432.3	0	93.16
4	301324.9	2916.9	198.8	20.2
5	264839.2	2430.2	0	0

Case 5: CCS, PtG, DR program, and TCSC-based FACTS devices are integrated into the test system. The reactance changes ratio by FACTS device and participation rate of consumers in the DR program is set to 40% and 5%, respectively. Results of Cases 1–5 are presented in Table 6. A comparison of these results shows that simultaneous usage of stated technologies leads to more decrease in total cost and carbon emissions. Unlike Cases 2, 3, and 4 (in which WEG is curtailed and electrical load is shed), in Case 5 all available WEG is accommodated,

and also electrical load is fully met. In Figures 13 and 14, hourly scheduling of G1 (cheapest unit) and G2 (most expensive unit) in Cases 1 and 5, are presented. These figures show that in Case 5 hourly power generation of G1 is increased and of G2 is decreased. However, a power generation portion of G1 is consumed by CCS in Case 5. As well, the NG wells' total output in Cases 1–5 is presented in Figure 15, which this value has decreased in Case 5 compared to Cases 1–4. This is due to the simultaneous use of flexible technologies, which leads to increased WEG penetration and NG production by PtG technology.

Case 6: The uncertainties posed by the DR program are handled with the IGD method. Different optimal values are obtained for the robustness function with changing Δr from 0 to 0.1. Figure 16 shows the changes in optimum robustness function with regards to Δr without and with flexible resources. It is obvious that Δr has a high impact on the optimum robustness function. For example, for $\Delta r = 0.02$ and $\Delta r = 0.08$, the value of the robustness function (with flexible resources) is 0.0456 and 0.0584, respectively. On the other hand, the values of the robustness function with flexible resources are very high compared to those without flexible resources. Therefore, it can be said that with flexible resources, a wide range of uncertainty can be managed, and DR uncertainty has a lower impact on the operation of IEGS.

5.2 | 24-bus power system with 10-node gas network

24-bus/10-node IEGS is used here as a large-scale test system. Figure 17 depicts this test system according to [16] and

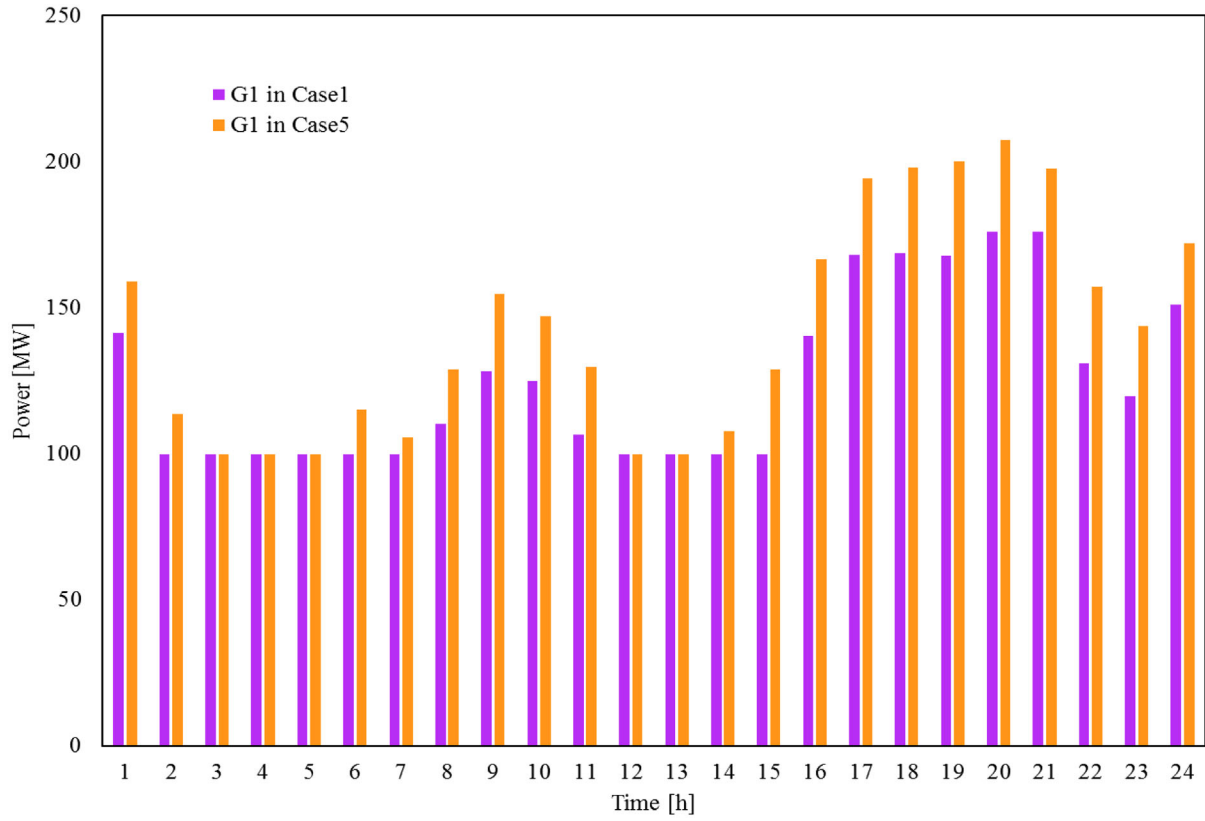


FIGURE 13 Hourly scheduling of G1 in Cases 1 and 4.

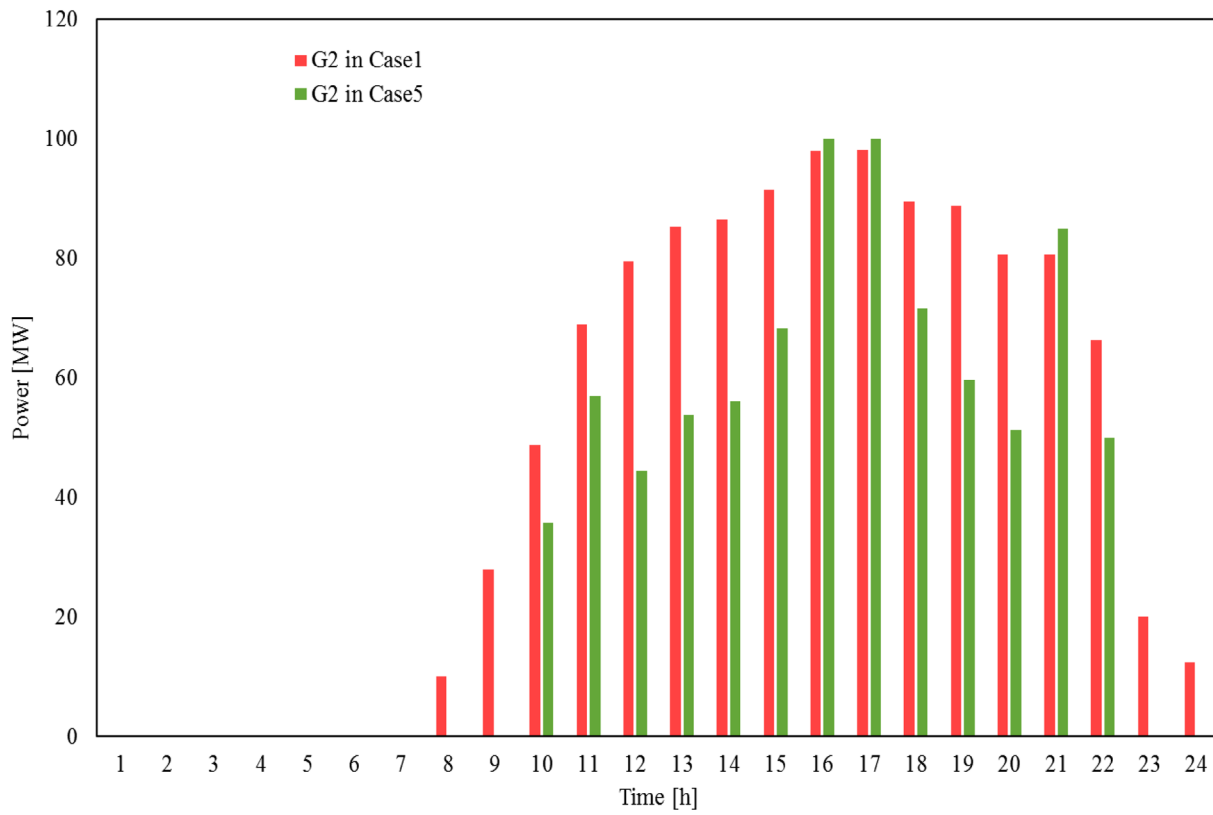


FIGURE 14 Hourly scheduling of G2 in Cases 1 and 4.

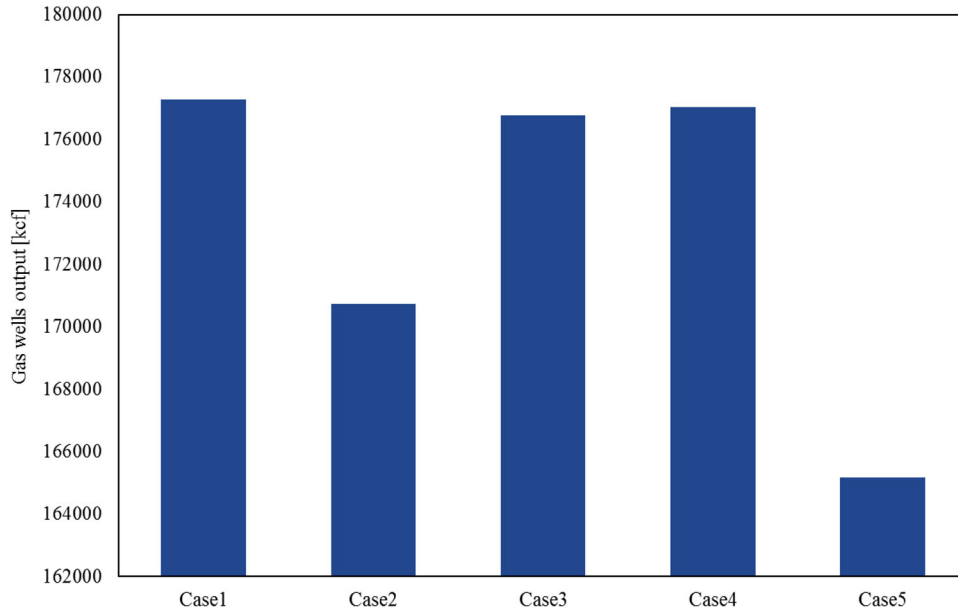


FIGURE 15 Natural gas wells total production in Cases 1–5.

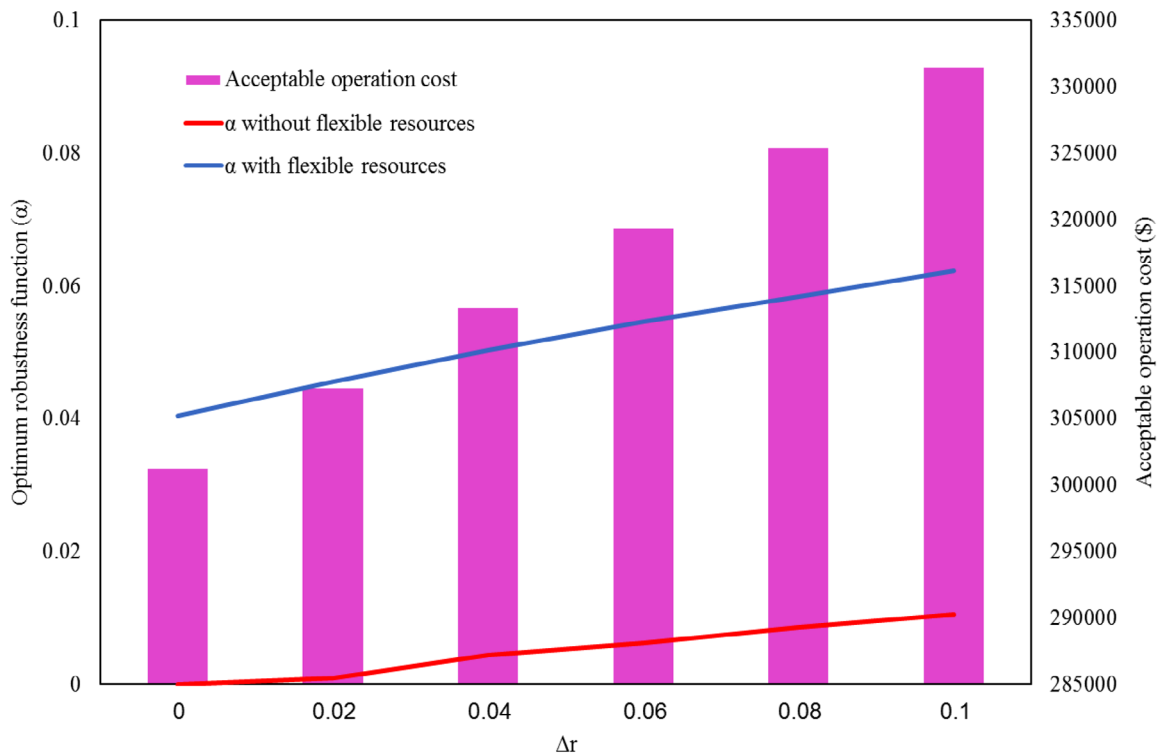


FIGURE 16 Variation of optimum robustness function against Δr .

[40]. The gas network contains three gas wells, seven loads, and ten pipelines. The power system contains seventeen loads, two WEGs, three GFGs (G1, G11, and G12) and nine non-GFGs. All non-GFGs are outfitted with CCS. Two PtGs are located in nodes 7 and 10 of the gas network and buses 17 and 21 of the power system. Additionally, two TCSC devices

are inserted in lines (16-17) and (15-21) of the power system. The carbon emission coefficients for GFGs and non-GFGs are 0.65 tCO₂/MWh and 0.85tCO₂/MWh, respectively. Technical specifications of CCSs and PtGs are similar to the 6-bus/6-node IEGS. All required data related to this test system can be found in [16] and [40].

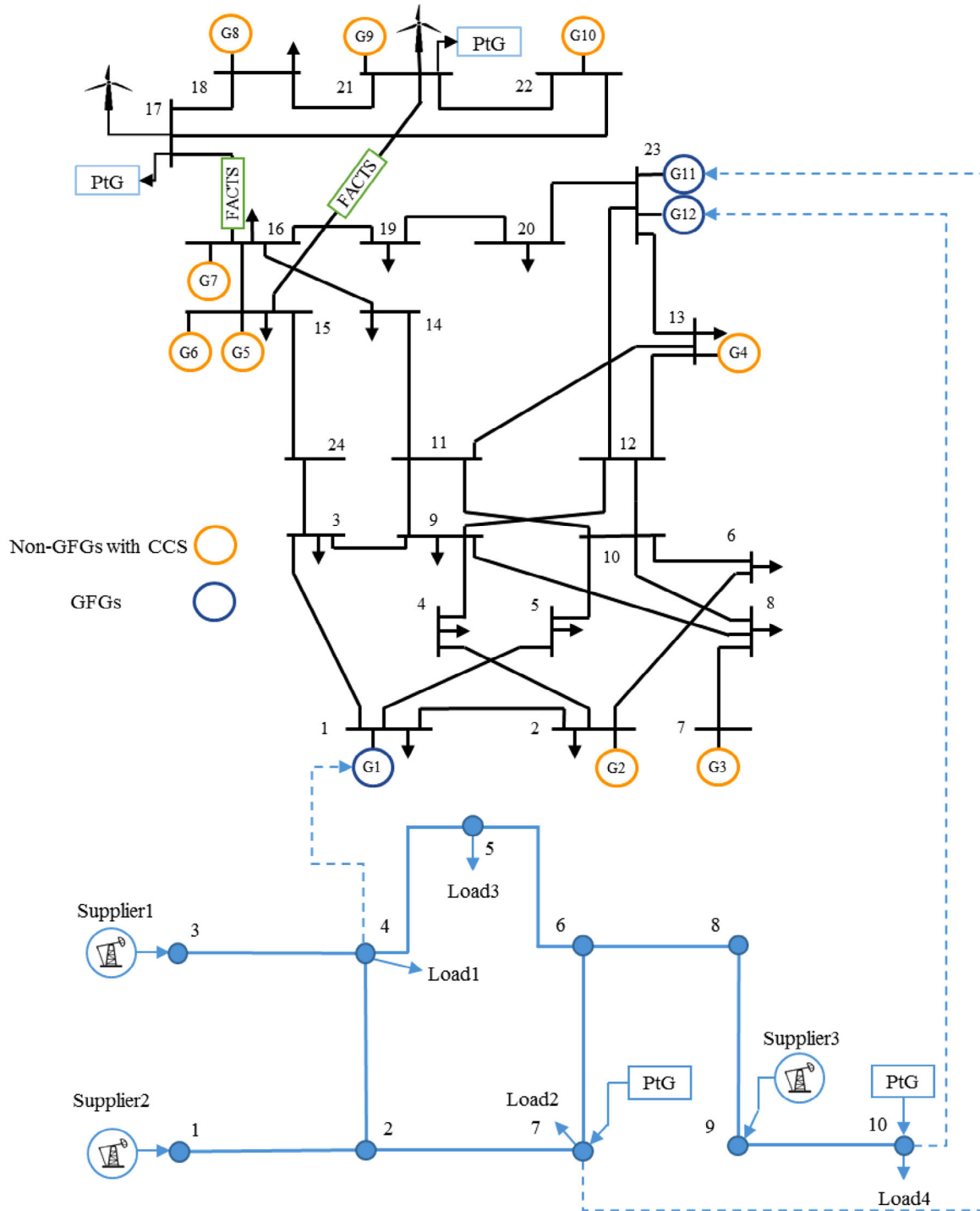


FIGURE 17 Large-scale test system.

The simulation results of cases 1–5 for the large-scale test system are summarized in Table 7. It is obvious that the high cost, high emission, high WPG curtailment, and high load shedding are related to case 1. On the other hand, the integration of each of the flexibility resources into the test system has decreased the four main objectives mentioned. However, by simultaneously integrating flexible resources into the test system, the total

cost and emissions have been further reduced, and the amount of load shedding and WPG curtailment is zero. To model the uncertainty of the DR program with the IGDT method, various strategies have been considered by changing Δr from 0 to 0.1. The effect of changing Δr on the optimum robustness function with and without flexibility resources is depicted in Figure 18. Based on this figure, α has increased with increasing Δr . In

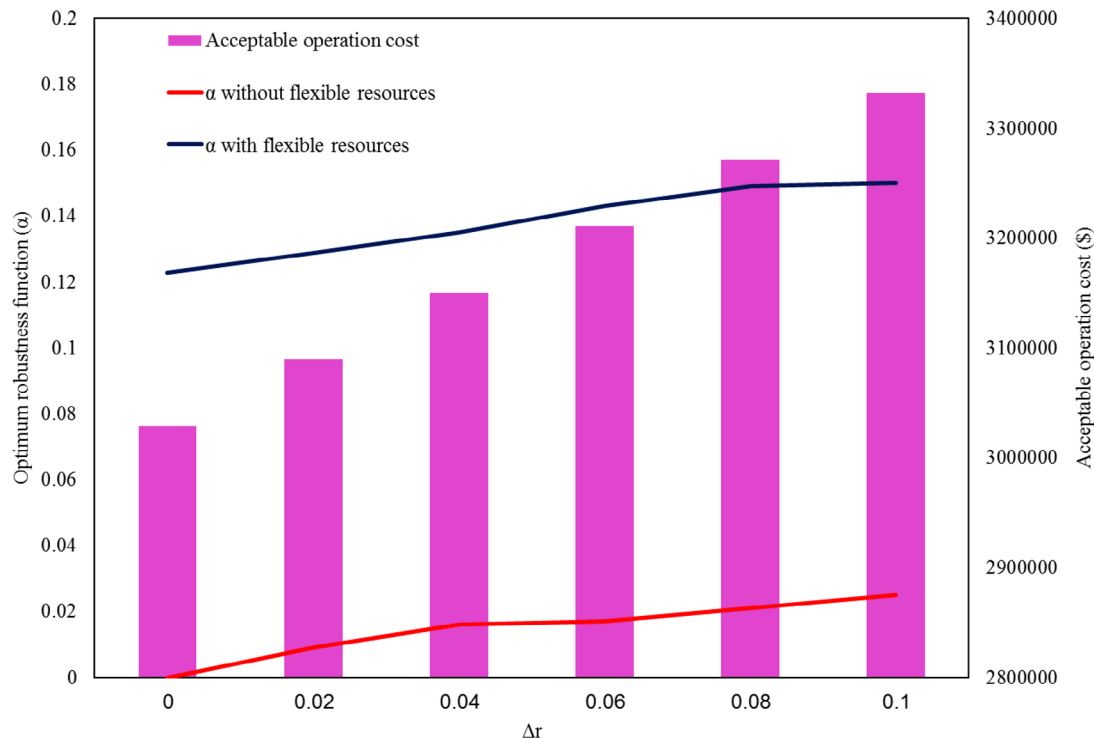


FIGURE 18 Variation of optimum robustness function against Δr .

TABLE 7 Results of cases 1–5 for the large-scale test system.

Case	Total cost (\$)	Total emission (tCO ₂)	WEG curtailment (MWh)	Electrical load shedding (MWh)
1	3029333.7	33694.7	433.9	1499.6
2	2823654.6	33669.7	191.4	1295.5
3	2511343.6	31100.6	0	1000.03
4	2678315.1	33767.5	193.5	1147.2
5	1510261.1	30543.6	0	0

addition, the value of α is high with flexibility resources, which means that flexibility resources are effective in compensating for the uncertainty of the DR program.

6 | CONCLUSIONS

This paper has presented a low-carbon ED model for IEGSs, in which flexibility from the generation side (GFG and CCS), network side (TCSC-based FACTS device and line pack), demand side (DR program), and storage side (PtG) is considered to support the environment-friendly and low-cost operation. To manage WEG's uncertainty, a two-stage stochastic methodology is proposed in which the uncertainties are modelled as a set of scenarios in the second stage. Also, uncertainty posed by the DR program is managed with the IGDT approach. The PtG system is equipped with HSF to further decrease the

IEGSs operation cost. To improve the computational burden, the presented MINLP model is converted and formulated as a MILP problem. The obtained results show that individual use of TCSC-based FACTS device (Case 2) cannot accommodate all WEG power. On the other hand, individual PtG system utilization (Case 3), can absorb all available WEG power but it could not prevent electrical load shedding. Also, with the DR program (Case 4) there is still WEG curtailment and load shedding. However, with the presented model (Case 5), all available WEG power is absorbed and the electrical load is fully met. Accordingly, not only carbon emissions and the overall cost of IEGSs are decreased but also the WEG penetration is increased. In this regard, the total cost, carbon emissions, and wind curtailment are decreased by 29%, 16.4%, and 100%, respectively, in the 6-bus/6-node IEGS. Results also show that line pack enhances the flexibility of the NG system and reduces total cost. Moreover, with these flexible resources, the uncertainty of the DR program has a lower impact on the low-carbon operation of IEGS. For future works, distributionally robust optimization can be used to cover uncertainties. The gas DR program and its uncertainty can also be considered in the low-carbon operation of IEGS.

NOMENCLATURE

Abbreviations

GHGs	Greenhouse gases
WEG	Wind energy generation
CCS	Carbon capture and storage
IEGSs	Integrated electricity-gas systems

FACTS	Flexible AC transmission system								capture rate of CCS [%]
DR	Demand response								
FFPPs	Fossil-fuel power plants							$P_i^{bs,CCS}$	Base power consumption of CCS technology i [MW]
CPPs	Conventional power plants								
NG	Natural gas								
ED	Economic dispatch							η^{PtG}	Power to hydrogen efficiency of PtG technology [%]
ESSs	Energy storage systems								
IGDT	Information gap decision theory								
CSF	CO ₂ storage facility							$P_m^{bs,ptg}$	Power consumption rate for the produced H ₂ of electrolyser m [MWh/kcf]
REs	Renewable energies								
GFG	Gas-fuel generator							$\lambda^{H_2-CO_2}/\mu^{H_2-CH_4}$	Sabatier reaction coefficients of H ₂ to CO ₂ /CH ₄
GETs	Grid-enhancing technologies								
ED	Economic dispatch								
MILP	Mixed-integer linear programming								
PDF	Probability distribution function								
CCPPs	Carbon-capture power plants							$P_{t,k}^{FWT}$	Forecasted power of WT k at hour t [MW]
WT	Wind turbine							$V^{ci}, V^{co}, V^{rated}$	Cut-in, cut-out, rated wind speed [m/s]
UC	Unit commitment							$V_{t,k}^{WT}$	Wind speed of WT k at hour t [m/s]
TCSC	Thyristor-controlled series capacitor							$P^{WT,rated}$	Rated power of WT [MW]
PtG	Power-to-gas								
HHV	Higher heating value								
HSF	H ₂ storage facility							$P_m^{Min,ptg}/P_m^{Max,ptg}$	Minimum, maximum consumption power of PtG technology m [MW]

Parameters

	HHV _{gas}	Higher heating value of NG [MBtu/kcf]							
	a_i, b_i	Cost coefficients of power plant i [MBtu/MWh], [MBtu]						$G_s^{S,in,Min}, G_s^{S,in,Max}$	Minimum, maximum injection rate of CO ₂ in CSF (or H ₂ in HSF) s [kcf/h]
	su_i^X, sd_i^X	Start-up, shut down fuel rate of generation units i [MBtu]						$G_s^{S,out,Min}, G_s^{S,out,Max}$	Minimum, maximum withdrawal rate of CO ₂ in CSF (or H ₂ in HSF) s [kcf/h]
	$P_i^{Min,X}, P_i^{Max,X}$	Minimum, maximum generating power of generation units i [MW]						Δt	Time interval [1h]
	$R_i^{UP,X}, R_i^{DN,X}$	Ramp up, ramp down rates of generation units i [MW/h]						M	Sufficient enough large constant used in the Big-M linearization method
	MUP _{i} , MDN _{i}	Minimum up-time, minimum down-time of generation units i [h]						$GL_s^{S,Min}, GL_s^{S,Max}$	Minimum, maximum capacity of CO ₂ in CSF (or H ₂ in HSF) s [kcf]
	RUP _{i} , RDN _{i}	Required up-time, down time of generation units i at the start of planning horizon [h]						$GL_{s,t=0}^{CO_2}, GL_{s,t=NT}^{CO_2}/GL_{s,t=0}^{H_2}, GL_{s,t=NT}^{H_2}$	First and final amount of CO ₂ in CSF s /H ₂ in HSF s [kcf]
	$\eta^X/\gamma^{CCS}/\kappa^{CCS}$	Emission intensity of generation units i [tCO ₂ /MWh]/ power consumption rate of carbon treatment [MWh/tCO ₂]/ carbon						$\mu^{CPP}/\mu^{CCPP}/\mu^{GFG}$	Carbon emission tax price of CPP/CCPP/GFG [\$/tCO ₂]
								$\mu^{ex,gw}$	Extraction price of the NG from the NG wells [\$/kcf]

$G_{gw}^{ex,gw,Min}, G_{gw}^{ex,gw,Max}$	Minimum, maximum NG extraction from the NG wells gw [kcf]
σ^{curt}	Curtailed electrical demand price [\$/MWh]
$GD_{g,t}$	NG demand g at hour t [kcf]
$ED_{d,t}^{bf}/ED_{d,t}^{af}$	Electrical demand d before/after the DR program [MW]
$B_l^{sus}/B_{lFACTS}^{sus}$	Susceptance of power system transmission line l without FACTS devices/line l^{FACTS} with FACTS devices [S]
pf_l^{Max}	Maximum power flow via transmission line l without FACTS devices [MW]
$DR_{d,t}^{max}$	Maximum participation of load in the DR program
$B_{lFACTS}^{sus,Min}, B_{lFACTS}^{sus,Max}$	Minimum, maximum susceptance of line l^{FACTS} with FACTS devices [S]
κ_{ef}^{ct}	NG flow constant of pipeline e, f [kcf/psig.h]
pr_e^{Min}, pr_e^{Max}	Minimum, maximum pressure at node e [psig]
$pr_{e,\vartheta}^{ct}$	Steady pressure point ϑ at node e [psig]

Indices/sets

$i/\psi_{CPP}, \psi_{CCPP}, \psi_{GFG}$	Index/set of CPP, CCPP, GFG
t	Index of hours
m/ψ_{ptg}	Index/set of PtG technology
k/ψ_{WT}	Index/set of WT
$s/\psi_{CSF}, \psi_{HSF}$	Index/set of CSF, HSF
gw/ψ_{GW}	Index/set of NG wells
l/ψ_L	Index/set of power system transmission lines without FACTS devices
l^{FACTS}/ψ_{lFACTS}	Index/set of power system transmission lines with FACTS devices
d/ψ_{ED}	Index/set of electrical demand
g/ψ_{GD}	Index/set of NG demand
ω/ψ_W	Index/set of considered scenarios
$b, b'/\psi_B$	Index/set of power system buses
$e, f/\psi_Z$	Index/set of NG system pipelines
e/ψ_E	Index/set of NG system nodes

ϑ/ψ_V	Index/set of steady pressure points for the linearization of the Weymouth non-linear equation
$edr_{d,t}$	Amount of load participated in DR program [MW]

Variables

$FFC_{i,t}(P_{i,t}^{out,X})$	Fuel consumption function for generation units i at hour t [kcf]
$P_{i,t}^{out,X}/P_{i,t}^{net,CCPP}$	Output power generation units i /net power of CCPP i at hour t [MW]
$SUC_{i,t}^X, SDC_{i,t}^X$	Start-up, shut down fuel of generation units i at hour t [MBtu]
$I_{i,t}^X$	Commitment status of generation units i at hour t
$Y_{i,t}, Z_{i,t}$	Binary variables to represent the start-up, shut down status of generation units i at hour t
$Em_{i,t}^X/Em_{i,t}^{net,CCPP}$	Carbon emitted by generation units i /net carbon emission by CCPP i at hour t [tCO ₂]
$Em_{i,t}^{tre,CCS}/Em_{i,t}^{tcc}$	Carbon treated/total captured carbon by CCPP i at hour t [tCO ₂]
$P_{i,t}^{cons,CCS}/P_{i,t}^{op,CCS}$	Consumption power /operational power of CCS i at hour t [MW]
$P_{m,t}^{ptg}$	Input power of PtG m at hour t [MW]
$H_{m,t}^{ptg}/H_{m,t}^{ptg,M}$	Produced H ₂ of electrolyser in PtG m /required H ₂ for the methanation process in PtG m at hour t [kcf]
$G_{m,t}^{CO_2}/G_{m,t}^{CH_4}$	Required CO ₂ /produced CH ₄ for the methanation process in PtG m at hour t [kcf]
$P_{t,k}^{WT}$	Power dispatch of WT k at hour t [MW]
$G_{s,t}^{S,in}, G_{s,t}^{S,out}$	Injection, withdrawal amount of CO ₂ in CSF (or H ₂ in HSF) s at hour t [kcf]
$I_{s,t}^{S,in}, I_{s,t}^{S,out}$	Commitment status of injection, withdrawal amount of CO ₂ in CSF (or H ₂ in HSF) s at hour t
$GL_{s,t}^S$	Available amount of CO ₂ in CSF (or H ₂ in HSF) s at hour t [kcf]
$G_{gw,t}^{ex,gw}$	Extracted NG from the NG wells gw at hour t [kcf]
$ED_{d,t}^{curt}$	Curtailed electrical demand d at hour t [MW]
$FFC_{i,t,\omega}^{sd}(P_{i,t,\omega}^{sd,out,X})$	Fuel consumption function for generation units i at hour t in scenario ω [kcf]
$Em_{i,t,\omega}^{sd,X}/Em_{i,t,\omega}^{sd,net,CCPP}$	Carbon emitted by generation units i /net carbon emission by CCPP at hour t in scenario ω [tCO ₂]
$G_{gw,t,\omega}^{sd,ex,gw}$	Extracted NG from the NG wells gw at hour t in scenario ω [kcf]

$ED_{d,t,\omega}^{\text{sd,curt}}$	Curtailed electrical demand d at hour t in scenario ω [MW]
$\rho f_{l,t}/\rho f_{l,\text{FACTS},t}$	Power flow via transmission line l without FACTS devices/ transmission line l^{FACTS} with FACTS devices at hour t [MW]
$G_{ef,t}^f, G_{ef,t}^{\text{in}}, G_{ef,t}^{\text{out}}$	NG flow/inflow/outflow of a pipeline e, f at hour t [kcf]
$L_{ef,t}^f$	Line pack of a pipeline e, f at hour t [kcf]
$\delta_{b,t}$	Voltage angle of power system bus b at hour t [rad]

AUTHOR CONTRIBUTIONS

Amir Talebi: Simulation and analysis; writing original draft. **Masoud Agabalaye-Rahvar:** Mathematical modelling; investigation; writing original draft. **Behnam Mohammadi-Ivatloo:** Methodology; writing—review and editing; results evaluating. **Kazem Zare:** Writing—review and editing; results evaluating. **Amjad Anvari-Moghaddam:** Validation; writing—review and editing. All authors have read and agreed to the published version of the manuscript.

CONFLICT OF INTEREST STATEMENT

The authors declare no conflicts of interest.

DATA AVAILABILITY STATEMENT

Data derived from public domain resources; the data that support the findings of this study are available in the references [16, 29, 39, 40]. These data were derived from the following resources available in the public domain.

ORCID

Masoud Agabalaye-Rahvar  <https://orcid.org/0000-0002-2677-6910>

Kazem Zare  <https://orcid.org/0000-0003-4729-1741>

REFERENCES

- Azimian, M., Amir, V., Javadi, S.: Economic and environmental policy analysis for emission-neutral multi-carrier microgrid deployment. *Appl. Energy* 277, 115609 (2020)
- U.S. Department of Energy: Advancing innovation, technology transitions, and early investments, U.S. Department of Energy. [Online]. Available: <https://www.energy.gov/topics/advancing-innovation-technology-transitions-and-early-investments>. Accessed 10 Jan 2022
- Esmaili, M., Ghamsari-Yazdel, M., Amjadi, N., Chung, C., Conejo, A.J.: Transmission expansion planning including TCSCs and SFCLs: a MINLP approach. *IEEE Trans. Power Syst.* 35(6), 4396–4407 (2020)
- Jalili, M., Holagh, S.G., Chitsaz, A., Song, J., Markides, C.N.: Electrolyzer cell-methanation/Sabatier reactors integration for power-to-gas energy storage: thermo-economic analysis and multi-objective optimization. *Appl. Energy* 329, 120268 (2023)
- Agabalaye-Rahvar, M., Mansour-Saatloo, A., Mirzaei, M.A., Mohammadi-Ivatloo, B., Zare, K., Anvari-Moghaddam, A.: Robust optimal operation strategy for a hybrid energy system based on gas-fired unit, power-to-gas facility and wind power in energy markets. *Energies* 13(22), 6131 (2020)
- Dancker, J., Wolter, M.: A coupled transient gas flow calculation with a simultaneous calorific-value-gradient improved hydrogen tracking. *Appl. Energy* 316, 118967 (2022)
- Zhao, C., Wang, J., Watson, J.-P., Guan, Y.: Multi-stage robust unit commitment considering wind and demand response uncertainties. *IEEE Trans. Power Syst.* 28(3), 2708–2717 (2013)
- Lucquiaud, M., Chalmers, H., Gibbins, J.: Potential for flexible operation of pulverised coal power plants with CO₂ capture. *Energy Mater.* 2(3), 177–183 (2008)
- Chen, Q., Kang, C., Xia, Q.: Modeling flexible operation mechanism of CO₂ capture power plant and its effects on power-system operation. *IEEE Trans. Energy Convers.* 25(3), 853–861 (2010)
- Chalmers, H., Lucquiaud, M., Gibbins, J., Leach, M.: Flexible operation of coal fired power plants with postcombustion capture of carbon dioxide. *J. Environ. Eng.* 135(6), 449–458 (2009)
- ReddyK, S., Panwar, L., Panigrahi, B., Kumar, R.: Low carbon unit commitment (LCUC) with post carbon capture and storage (CCS) technology considering resource sensitivity. *J. Cleaner Prod.* 200, 161–173 (2018)
- Lou, S., Lu, S., Wu, Y., Kirschen, D.S.: Optimizing spinning reserve requirement of power system with carbon capture plants. *IEEE Trans. Power Syst.* 30(2), 1056–1063 (2014)
- Fang, S., Xu, Y., Li, Z., Ding, Z., Liu, L., Wang, H.: Optimal sizing of ship-board carbon capture system for maritime greenhouse emission control. *IEEE Trans. Ind. Appl.* 55(6), 5543–5553 (2019)
- Ji, Z., et al.: Low-carbon power system dispatch incorporating carbon capture power plants. *IEEE Trans. Power Syst.* 28(4), 4615–4623 (2013)
- Akbari-Dibavar, A., Mohammadi-Ivatloo, B., Zare, K., Khalili, T., Bidram, A.: Economic-emission dispatch problem in power systems with carbon capture power plants. *IEEE Trans. Ind. Appl.* 57, 3341–3351 (2021)
- Akhlaghi, M., Moravej, Z., Bagheri, A.: Maximizing wind energy utilization in smart power systems using a flexible network-constrained unit commitment through dynamic lines and transformers rating. *Energy* 261, 124918 (2022)
- Nasri, A., Conejo, A.J., Kazempour, S.J., Ghandhari, M.: Minimizing wind power spillage using an OPF with FACTS devices. *IEEE Trans. Power Syst.* 29(5), 2150–2159 (2014)
- Sang, Y., Sahraei-Ardakani, M.: The interdependence between transmission switching and variable-impedance series FACTS devices. *IEEE Trans. Power Syst.* 33(3), 2792–2803 (2017)
- Luburić, Z., Pandžić, H.: FACTS devices and energy storage in unit commitment. *Int. J. Electr. Power & Energy Syst.* 104, 311–325 (2019)
- Nikoobakht, A., Aghaei, J., Mokarram, M.J., Shafie-khah, M., Catalão, J.P.: Adaptive robust co-optimization of wind energy generation, electric vehicle batteries and flexible AC transmission system devices. *Energy* 230, 120781 (2021)
- He, L., Lu, Z., Zhang, J., Geng, L., Zhao, H., Li, X.: Low-carbon economic dispatch for electricity and natural gas systems considering carbon capture systems and power-to-gas. *Appl. Energy* 224, 357–370 (2018)
- Liu, X., Li, X., Tian, J., Cao, H.: Low-carbon economic dispatch of integrated electricity and natural gas energy system considering carbon capture device. *Trans. Inst. Meas. Control* 11, 25077–25089 (2021)
- Shengnan, R., Jin, W., Xiaoqing, G., Luowen, G., Peng, X., Ao, J.: Low-carbon economic dispatching for integrated energy system based on coordinated optimization of power to gas and carbon capture power plant. In: 2019 IEEE 3rd Conference on Energy Internet and Energy System Integration (EI2), pp. 39–43. IEEE, Piscataway, NJ (2019)
- Qing, Y., et al.: Low-carbon coordinated scheduling of integrated electricity-gas distribution system with hybrid AC/DC network. *IET Renewable Power Gener.* 16, 2566–2578 (2022)
- Xu, Y., Ding, T., Qu, M., Wen, Y., Ning, Y.: Low-carbon power system economic dispatch considering renewable energy accommodation. In: 8th Renewable Power Generation Conference (RPG 2019), pp. 1–8. IET, London (2019)
- Ma, Y., et al.: Modeling and optimization of combined heat and power with power-to-gas and carbon capture system in integrated energy system. *Energy* 236, 121392 (2021)
- Wang, Y., Gao, S., Jia, W., Ding, T., Zhou, Z., Wang, Z.: Data-driven distributionally robust economic dispatch for park integrated energy systems with coordination of carbon capture and storage devices and combined heat and power plants. *IET Renewable Power Gener.* 16, 2617–2629 (2022)

28. Xiang, Y., et al.: Low-carbon economic dispatch of electricity-gas systems. *Energy* 226, 120267 (2021)
29. Cao, Z., Wang, J., Zhao, Q., Han, Y., Li, Y.: Decarbonization scheduling strategy optimization for electricity-gas system considering electric vehicles and refined operation model of power-to-gas. *IEEE Access* 9, 5716–5733 (2021)
30. Nasiri, N., et al.: A robust bi-level optimization framework for participation of multi-energy service providers in integrated power and natural gas markets. *Appl. Energy* 340, 121047 (2023)
31. Alabi, T.M., Lu, L., Yang, Z.: Data-driven optimal scheduling of multi-energy system virtual power plant (MEVPP) incorporating carbon capture system (CCS), electric vehicle flexibility, and clean energy marketer (CEM) strategy. *Appl. Energy* 314, 118997 (2022)
32. Owebor, K., Diemuodeke, E., Briggs, T.: Thermo-economic and environmental analysis of integrated power plant with carbon capture and storage technology. *Energy* 240, 122748 (2022)
33. Parra, D., Zhang, X., Bauer, C., Patel, M.K.: An integrated techno-economic and life cycle environmental assessment of power-to-gas systems. *Appl. Energy* 193, 440–454 (2017)
34. Mirzaei, M.A., Ahmadian, A., Mohammadi-Ivatloo, B., Zare, K., Elkamel, A.: A mixed conditional value-at-risk/information gap decision theory framework for optimal participation of a multi-energy distribution system in multiple energy markets. *J. Cleaner Prod.* 371, 133283 (2022)
35. Sahraei-Ardakani, M., Hedman, K.W.: A fast LP approach for enhanced utilization of variable impedance based FACTS devices. *IEEE Trans. Power Syst.* 31(3), 2204–2213 (2015)
36. Wang, J., Xin, H., Xie, N., Wang, Y.: Equilibrium models of coordinated electricity and natural gas markets with different coupling information exchanging channels. *Energy* 239, 121827 (2022)
37. Ordoudis, C., Pinson, P., Morales, J.M.: An integrated market for electricity and natural gas systems with stochastic power producers. *Eur. J. Oper. Res.* 272(2), 642–654 (2019)
38. Sun, Q., Fu, Y., Lin, H., Wennersten, R.: A novel integrated stochastic programming-information gap decision theory (IGDT) approach for optimization of integrated energy systems (IESs) with multiple uncertainties. *Appl. Energy* 314, 119002 (2022)
39. Talebi, A., Sadeghi-Yazdankhah, A., Mirzaei, M.A., Mohammadi-Ivatloo, B.: Co-optimization of electricity and natural gas networks considering ac constraints and natural gas storage. In: 2018 Smart Grid Conference (SGC), pp. 1–6. IEEE, Piscataway, NJ (2018)
40. Alabdulwahab, A., Abusorrah, A., Zhang, X., Shahidehpour, M.: Stochastic security-constrained scheduling of coordinated electricity and natural gas infrastructures. *IEEE Syst. J.* 11(3), 1674–1683 (2017)

How to cite this article: Talebi, A., Agabalaye-Rahvar, M., Mohammadi-Ivatloo, B., Zare, K., Anvari-Moghaddam, A.: An IGDT-stochastic model for low-carbon economic dispatch of integrated electricity-natural gas systems considering grid-enhancing technologies. *IET Gener. Transm. Distrib.* 1–23 (2024).
<https://doi.org/10.1049/gtd2.13327>

APPENDIX

TABLE A1 Parameters of generators [39].

Gen	R^{UP}, R^{DN}		P^{min} (MW)	MUP (h)	MDN (h)	MUP ⁱⁿⁱ (h)	MDN ⁱⁿⁱ (h)	a (MBtu/MWh)	b (MBtu/h)
	(MW/h)	P^{max} (MW)							
G1	55	220	100	4	4	4	0	13.5	176.9
G2	50	100	10	2	3	0	3	32.6	129.9
G3	20	20	10	1	1	0	1	17.7	137.4

TABLE A2 Parameters of gas network [39].

Node	Pressure bound		Gas wells' data		Pipelines' data	
	Min (Psig)	Max (Psig)	Min (kcf/h)	Max (kcf/h)	Receiving node	κ_{ef}^{ct} (kcf/Psig)
1	105	120	–	–	2	50.6
2	120	135	–	–	4	50.1
3	125	140	–	–	5	43.5
4	130	155	1500	5000	–	–
5	140	155	–	–	2	37.5
6	150	175	2000	6000	5	45.3

TABLE A3 Parameters of HSF.

Min capacity (kcf)	Max capacity (kcf)	Max charge (kcf/h)	Max discharge (kcf/h)
150	1500	300	300